SCISPACE
formerly Typeset

Open access • Posted Content • DOI:10.1101/616961

B-lactamase Amplification and Porin Loss Drive Progressive β-lactam Resistance in Recurrent ESBL Enterobacteriaceae Bacteremia — Source link

William C Shropshire, Samuel L. Aitken, Samuel L. Aitken, Reed Pifer ...+14 more authors

Institutions: University of Texas Health Science Center at Houston, University of Texas MD Anderson Cancer Center, University of Texas Southwestern Medical Center, El Bosque University

Published on: 23 Apr 2019 - bioRxiv (American Society of Hematology)

Topics: Carbapenem-resistant enterobacteriaceae

Related papers:

- Concurrence of Porin Loss and Modular Amplification of β-Lactamase Encoding Genes Drives Carbapenem Resistance in a Cohort of Recurrent Enterobacterales Bacteremia
- IS26-mediated amplification of blaOXA-1 and blaCTX-M-15 with concurrent outer membrane porin disruption associated with de novo carbapenem resistance in a recurrent bacteraemia cohort
- Carbapenem Resistance Caused by High-Level Expression of OXA-663 β-Lactamase in an OmpK36-Deficient Klebsiella pneumoniae Clinical Isolate.
- Presence of different beta-lactamase classes among clinical isolates of Pseudomonas aeruginosa expressing AmpC beta-lactamase enzyme.
- Alarming β-lactamase-mediated resistance in multidrug-resistant Enterobacteriaceae.

Share this paper:

View more about this paper here: https://typeset.io/papers/b-lactamase-amplification-and-porin-loss-drive-progressive-b-4s1z1w1zy5

bioRxiv preprint doi: https://doi.org/10.1101/616961; this version posted March 19, 2020. The copyright holder for this preprint (which was not certified by peer review) is the author/funder. All rights reserved. No reuse allowed without permission.

Concurrence of Porin Loss and Modular Amplification of β-Lactamase Encoding Genes Drives Carbapenem Resistance in a Cohort of Recurrent *Enterobacterales* Bacteremia

William C. Shropshire[1,2], Samuel L. Aitken[2,3], Reed Pifer[4], Jiwoong Kim[5], Micah M. Bhatti[6], Xiqi Li[7], Awdhesh Kalia[8], Jessica Galloway-Peña[2,7,9], Pranoti Sahasrabhojane[7], Cesar A. Arias[1,2,10,11], David E. Greenberg[2,12,13], Blake M. Hanson[1,2], Samuel A. Shelburne[2,7,9]#

[1]Center for Infectious Diseases, School of Public Health, University of Texas Health Science Center, Houston, Texas, USA

[2]Center for Antimicrobial Resistance and Microbial Genomics, Division of Infectious Diseases, University of Texas McGovern Medical School at Houston, Houston, Texas, USA

[3]Division of Pharmacy, MD Anderson Cancer Center, Houston, Texas, USA

[4]Division of Infectious Diseases, Department of Internal Medicine, University of Texas McGovern Medical School at Houston, Houston, Texas, USA

[5]Department of Bioinformatics, UT Southwestern Medical Center, Dallas, Texas, USA

[6]Department of Laboratory Medicine, MD Anderson Cancer Center, Houston, Texas, USA

[7]Department of Infectious Diseases, MD Anderson Cancer Center, Houston, Texas, USA

[8]Graduate Program in Diagnostic Genetics, School of Health Professions, The University of Texas M.D. Anderson Cancer Center, Houston, Texas, USA

[9]Department of Genomic Medicine, MD Anderson Cancer Center, Houston, Texas, USA

bioRxiv preprint doi: https://doi.org/10.1101/616961; this version posted March 19, 2020. The copyright holder for this preprint (which was not certified by peer review) is the author/funder. All rights reserved. No reuse allowed without permission.

[10]Department of Microbiology and Molecular Genetics, University of Texas McGovern Medical School at Houston, Houston, Texas, USA

[11]Molecular Genetics and Antimicrobial Resistance Unit-International Center for Microbial Genomics, Universidad El Bosque, Bogotá, Colombia.

[12]Department of Internal Medicine, UT Southwestern, Dallas, Texas, USA

[13]Department of Microbiology, UT Southwestern, Dallas, Texas, USA

#Address correspondence to Samuel A. Shelburne, MD, PhD, sshelburne@mdanderson.org

bioRxiv preprint doi: https://doi.org/10.1101/616961; this version posted March 19, 2020. The copyright holder for this preprint (which was not certified by peer review) is the author/funder. All rights reserved. No reuse allowed without permission.

ABSTRACT

Background

Carbapenem resistant *Enterobacterales* (CRE) remain urgent antimicrobial resistance threats. Approximately half of CRE clinical isolates lack carbapenem hydrolyzing enzymes and develop carbapenem resistance through alternative mechanisms. The purpose of this study was to elucidate the development of carbapenem resistance mechanisms from clonal, recurrent extended-spectrum β-lactamase positive *Enterobacterales* (ESBL-E) bacteremia isolates in a vulnerable patient population.

Methods

This study investigated a historical, retrospective cohort of ESBL-E bacteremia cases in the University of Texas MD Anderson Cancer Center (MDACC) from January 2015 to July 2016. Phylogenetic and comparative genomic analyses were performed to identify clonal, recurrent ESBL-E isolates developing carbapenem resistance. Oxford Nanopore Technology (ONT) long-read and Illumina short-read sequencing data were used to generate consensus assemblies and to identify signatures of mobile genetic element mediated amplification and transposition of antimicrobial resistance genes. Serial passaging experiments were performed on a set of clinical ST131 ESBL-E isolates to recapitulate *in vivo* observations. qPCR and qRT-PCR were used to determine respective copy number and transcript levels of β-lactamase genes.

Results

116 ESBL-E bacteremia cases were identified, 16 of which had documented recurrent infections. Four serial, recurrent isolates displayed a carbapenem resistant phenotype, three without the acquisition of a known carbapenemase. These three isolates had non-carbapenemase-producing CRE (non-CP-CRE) mechanisms driven by IS*26*- and IS*Ecp1*-mediated amplification of

bioRxiv preprint doi: https://doi.org/10.1101/616961; this version posted March 19, 2020. The copyright holder for this preprint (which was not certified by peer review) is the author/funder. All rights reserved. No reuse allowed without permission.

respective translocatable units (TU) and transposition units (TPU) harboring both *bla*$_{\text{OXA-1}}$ and *bla*$_{\text{CTX-M}}$ variants with concomitant outer membrane porin disruption. The TU and TPU structures inserted into the open reading frames of outer membrane porin genes in a subset of non-CP-CRE isolates. Serial passage of an index ST131 ESBL-E isolate under selective carbapenem exposure resulted in chromosomal amplification of modular, TUs harboring β-lactamase genes with concomitant porin inactivation, recapitulating the *in vivo* carbapenem resistance progression. Long-read sequencing of two additional MDACC bacteremia strains identified similar non-CP-CRE mechanisms observed in the serial isolates.

Conclusions

Non-CP-CRE *de novo* mechanisms were the primary driver of CRE development in recurrent bacteremia cases within this vulnerable patient population. The incorporation of long-read ONT data into AMR surveillance platforms is critical to identify high-risk CRE isolates that are difficult to identify with low-resolution phenotypic and molecular characterization methods.

Keywords:

Non-carbapenemase-producing carbapenem resistant *Enterobacterales*, Oxford Nanopore Technologies MinION Sequencing, Mobile Genetic Element Amplifications, Mobile Genetic Element Transpositions

bioRxiv preprint doi: https://doi.org/10.1101/616961; this version posted March 19, 2020. The copyright holder for this preprint (which was not certified by peer review) is the author/funder. All rights reserved. No reuse allowed without permission.

BACKGROUND

Antimicrobial resistance (AMR) is an emerging global health priority and carbapenem resistant *Enterobacterales* (CRE) are among the most serious AMR threats (1). Carbapenem resistance can develop due to the acquisition of enzymes that hydrolyze carbapenems, known as carbapenemases, as well as through changes in outer membrane permeability and/or drug efflux activity, which decrease intracellular carbapenem concentrations (2). While most CRE research has focused on characterizing carbapenemases (2), recent clinical and molecular epidemiology studies indicate approximately 50% of CRE isolates are not carbapenemase carriers, suggesting a substantial proportion of CRE isolates develop carbapenem resistance through alternative mechanisms (3, 4). Molecular characterization of these alternative mechanisms indicate non carbapenemase-producing carbapenem resistant *Enterobacterales* (non-CP-CRE) generally carry extended-spectrum β-lactamases (ESBL) or AmpC-like enzymes with concomitant mutations that alter porin function (2). Further studies reveal that *Enterobacterales* strains carrying outer membrane porin mutations, but lacking ESBL or AmpC-like enzymes, develop *de novo* carbapenem resistance at lower rates during serial passage under increasing carbapenem concentrations (5, 6). Thus, the presence of ESBL or cephalosporinase genes may be a component cause in non-CP-CRE development. Additionally, van Boxtel et al. demonstrated that serial passaging of an ESBL or AmpC-producing isolate in the presence of a carbapenem can result in amplification of plasmid-borne β-lactamase genes (7). Increased expression of the narrow-spectrum TEM β-lactamases has similarly been reported to result in cefepime (8) and piperacillin-tazobactam resistance (9-11), indicating that β-lactamase gene dosage is a factor in increasing resistance to multiple β-lactam chemotherapies. These findings demonstrate expression level and copy number of β-lactamases without known carbapenemase activity have

bioRxiv preprint doi: https://doi.org/10.1101/616961; this version posted March 19, 2020. The copyright holder for this preprint (which was not certified by peer review) is the author/funder. All rights reserved. No reuse allowed without permission.

95 important effects on carbapenem susceptibility in porin deficient backgrounds (6, 7).
96 Nevertheless, there remains a gap in knowledge regarding how these non-CP-CRE mechanisms
97 evolve *in vivo*, as few existing studies have investigated serially collected isolates from large,
98 patient cohorts (12-16).
99
100 This gap in knowledge is particularly relevant in carbapenem resistant *Escherichia coli*, where
101 the majority of these isolates are non-CP-CRE (3, 4). Additionally, *Klebsiella pneumoniae*
102 isolates with non-CP-CRE phenotypes have also been identified, albeit less frequently (3, 4).
103 Both non-CP-CR *E. coli* and *K. pneumoniae* can cause severe disease, including bacteremia,
104 which have high mortality rates (17). The detection and treatment of infections with these non-
105 CP-CRE isolates remain challenging relative to carbapenemase producing CRE as phenotypic
106 tests may incorrectly identify these isolates as carbapenem susceptible and definitive therapy
107 options may not be readily evident. This highlights the importance to further characterize non-
108 CP-CRE mechanism development, which may provide insights into new surveillance and/or
109 treatment options. Since there remains a lack of studies fully characterizing non-CP-CRE
110 development, we performed a systematic analysis of non-CP-CRE mechanisms using a large
111 cohort of patients with whole genome sequencing (WGS).
112
113 We utilized a cohort of patients with ESBL-E bacteremia from the University of Texas MD
114 Anderson Cancer Center (MDACC). Importantly, analysis of a previous MDACC cohort of non-
115 CP-CRE bacteremia isolates indicated these strains had increased short-read mapping of β-
116 lactamase encoding genes suggestive of β-lactamase encoding gene amplification (18).
117 Nevertheless, the amplification structures and genomic context of these gene amplifications

bioRxiv preprint doi: https://doi.org/10.1101/616961; this version posted March 19, 2020. The copyright holder for this preprint (which was not certified by peer review) is the author/funder. All rights reserved. No reuse allowed without permission.

could not be discerned with this short-read sequencing analysis. This is due to inherent limitations with short-read sequencing assemblers, which have difficulties resolving the complex, repetitive mobile genetic elements (MGEs) that carry resistance genes (19). Therefore, we present an analysis utilizing Oxford Nanopore Technologies (ONT) MinION sequencing, a long-read sequencing platform, which overcomes these limitations to elucidate these amplification mechanisms. This study aims to track the *de novo* development of carbapenem resistance mechanisms during recurrent *Enterobacterales* bacteremia infection by specifically focusing on ESBL positive *E. coli* and *K. pneumoniae* strains and characterizing the non-CP-CRE associated β-lactamase amplification mechanisms within our cohort.

METHODS

Study design and clinical data abstraction

A retrospective review of patients with ESBL-E bacteremia hospitalized from January 2015 to July 2016 was conducted at MDACC in Houston, Texas. All patients with one or more episodes of ESBL-E bacteremia who were 18 years of age or greater were eligible for inclusion. Blood culture isolates are routinely saved at MDACC and stored at -80°C. Clinical and demographic characteristics were manually extracted from electronic medical records and recorded using REDCap software (Vanderbilt University, Nashville, TN) (20).

Isolate identification and antimicrobial susceptibility testing

Antibiotic susceptibility testing was performed per routine clinical laboratory practice using an automated system (Vitek2, bioMérieux, Marcy L'Étoile, France) with additional testing performed as needed using individual antibiotic gradient strips (Etest, bioMérieux). ESBL

bioRxiv preprint doi: https://doi.org/10.1101/616961; this version posted March 19, 2020. The copyright holder for this preprint (which was not certified by peer review) is the author/funder. All rights reserved. No reuse allowed without permission.

141 production was assessed per routine laboratory practice on *E. coli*, *K. pneumonia*, and *K. oxytoca*
142 isolates that were resistant to one or more oxyimino-cephalosporins (e.g. cefotaxime,
143 ceftriaxone, or ceftazidime) using either the ESBL Etest (bioMérieux) or the Rapid ESBL Screen
144 kit (ROSCO, Taastrup, Denmark). Carbapenemase production was evaluated in the clinical lab
145 on any *Enterobacterales* isolate resistant to one more of the carbapenems using the Neo-Rapid
146 CARB kit (ROSCO) according to manufacturer's instructions. Carbapenem resistance (CR) was
147 defined as resistance to either ertapenem or meropenem using CLSI criteria (21). Recurrent
148 *Enterobacterales* bacteremia was defined as identification of the same species in blood culture at
149 any point during the follow-up period following at least one negative blood culture and
150 completion of an antibiotic treatment regimen.
151
152 **Illumina short-read sequencing**
153 All available isolates from recurrent bacteremia patients, initially underwent whole genome
154 sequencing (WGS) via Illumina HiSeq as described previously (18). The paired-end short-reads
155 were assessed using the FastQC toolkit (Babraham Institute), and adaptors as well as low-quality
156 reads were trimmed using Trimmomatic v0.33 (22). Genome assembly was performed using
157 SPAdes v3.9.1 (23). Depth of short read mapping to individual genes of interest was quantitated
158 relative to the average read mapping depth for the pubMLST housekeeping gene schema for *E.*
159 *coli* ST10 and ST131 respectively.
160
161 **Oxford Nanopore Technologies (ONT) long-read sequencing**
162 Serial isolates that developed non-CP-CRE, isolates used in the serial passaging experiments,
163 and non-CP-CRE isolates from a previous study (18) underwent Oxford Nanopore Technologies

bioRxiv preprint doi: https://doi.org/10.1101/616961; this version posted March 19, 2020. The copyright holder for this preprint (which was not certified by peer review) is the author/funder. All rights reserved. No reuse allowed without permission.

(ONT) long-read sequencing. Library preps were completed using the SQK-RBK004 rapid barcoding kit with ~400 ng of input DNA and run on ONT MinION R9.4.1 flow cells using the ONT GridION X5 (Oxford, UK) per manufacturer's instructions. ONT fast5 data was generated using ONT MinKNOW software (v3.0.13) with subsequent base-calling using Guppy v3.2.2 software (Oxford, UK). qcat-v1.1.0 was used for read demultiplexing, read length filtering (>1000 bp), and barcode removal (nanoporetech qcat GitHub: https://github.com/nanoporetech/qcat). A custom python script was used for the generation of polished, consensus assemblies (Shropshire, W flye_hybrid_assembly_pipeline GitHub: https://github.com/wshropshire/flye_hybrid_assembly_pipeline). Briefly, the Flye-v2.5 (24) assembler was used for *de novo* assembly, and contigs were circularized using berokka-v0.2 (Seemann, T berokka GitHub: https://github.com/tseemann/berokka). The circlator v1.5.5 (25) 'clean' command was then used to remove duplicate contigs sharing at least 90% identity. The remaining contigs were polished with Racon-v.1.4.5 (26) using the Oxford Nanopore long reads and then re-oriented with Circlator (25) "fixstart" to standardize the chromosome to the *dnaA* gene. A second long-read polish was then performed with Racon-v1.4.5 and these polished, corrected contigs were used as input for Medaka v0.8.1 long-read polishing (nanoporetech medaka GitHub: https://github.com/nanoporetech/medaka) followed by multiple rounds of Illumina short-read polishing using Racon-v1.4.5 (26). ONT assembly metrics are provided in **Table S1**.

Phylogenetics, genetic variant calling, and clonality analysis

Phylogenetic analysis, *in silico* MLST, and subsequent variant-calling of serial isolates compared against the index strain ONT consensus assembly were used to determine clonality. Initially, the

bioRxiv preprint doi: https://doi.org/10.1101/616961; this version posted March 19, 2020. The copyright holder for this preprint (which was not certified by peer review) is the author/funder. All rights reserved. No reuse allowed without permission.

pan-genome pipeline tool Roary-v3.12.0 (27) was used to perform a core genome alignment of the short-read SPAdes assemblies using the probabilistic alignment program PRANK (27, 28). A core genome pairwise SNP distance matrix was generated with these data using a custom Python script (Narechania, A GitHub:https://github.com/narechan/amnh/blob/master/bin/snp_matrixBuilder.pl), which was subsequently used to build a maximum likelihood (ML) phylogenetic tree using RAxML-v8.2.12 (29). *In silico* multi-locus sequencing typing (MLST) was performed on the short-read SPAdes assemblies using mlst-v2.15.1 (Seemann, T mlst Github: https://github.com/tseemann/mlst; (30). Recurrent isolates that became non-CP-CRE were checked for clonality using the variant calling pipeline tool Snippy-v4.3.6 (Seemann, T snippy GitHub: https://github.com/tseemann/snippy) with INDELs removed.

Genome annotation, AMR gene, and MGE identification

Gene calling and functional annotation was performed using Prokka-v1.14.0 (31). Annotated consensus genomes, as well as individual contigs, were parsed with ABRicate (Seemann, T ABRicate Github: https://github.com/tseemann/abricate) using the Comprehensive Antibiotic Resistance Database (CARD) (32) and PlasmidFinder (33) to search for AMR determinants and plasmid signatures respectively. Additionally, annotated Prokka gbk files were used to characterize ORFs of interests as well as confirm the results found with ABRicate. CARD, PlasmidFinder, ISFinder (34) and BLAST webtools were utilized during manual inspection of the assemblies to ensure correct context of annotated features, identify inverted repeat regions and target site duplications of insertion sequences, and confirm likely AMR gene mutations if present.

bioRxiv preprint doi: https://doi.org/10.1101/616961; this version posted March 19, 2020. The copyright holder for this preprint (which was not certified by peer review) is the author/funder. All rights reserved. No reuse allowed without permission.

In cases where assemblies were not completely resolved due to putative large repeat regions that could not be fully captured on ONT long reads, we used a newly developed tool SVAnts-v0.1 (35) (Hanson, Blake SVAnts Github: https://github.com/EpiBlake/SVAnts) to investigate subsets of ONT long reads. This tool enabled us to find individual ONT long reads containing MGEs of interest and align the DNA bordering these MGEs to our index assemblies to identify the regions in which the MGE was inserted within each bacterial genome.

B-lactamase encoding gene and gene transcript level analysis

Quantitative PCR (qPCR) and quantitative real-time PCR (qRT-PCR) was used to assess both DNA copy number and RNA transcript levels respectively. Strains were grown in triplicate on two separate days (six biologic replicates) to mid-exponential phase (OD_{600} ~ 0.5) in Luria-Bertani (LB) broth (ThermoFisher) at 37º C shaking at 220 rpm. DNA isolation was performed using the DNEasy kit (Qiagen) and qPCR was performed using TaqMan reagents on the StepOne Plus Real Time PCR platform (Applied Biosystems). The DNA levels of $bla_{\text{OXA-1}}$ and $bla_{\text{CTX-M}}$ were determined relative to the *rpsL* control gene using the ΔCt method (6).

For RNA transcript level analysis, cells were mixed 1:2 with RNAProtect (Qiagen) and harvested via centrifugation. RNA was isolated from cell pellets using the RNEasy kit (Qiagen) and converted to cDNA using the High Capacity cDNA Reverse Transcription Kit (Applied Biosystems). Relative transcript levels of the β-lactamase encoding genes ($bla_{\text{OXA-1}}$ and $bla_{\text{CTX-M}}$) were assayed using TaqMan reagents on the StepOne Plus Real Time PCR machine (Applied Biosystems). The transcript level of $bla_{\text{OXA-1}}$ and $bla_{\text{CTX-M}}$ were determined relative to the

bioRxiv preprint doi: https://doi.org/10.1101/616961; this version posted March 19, 2020. The copyright holder for this preprint (which was not certified by peer review) is the author/funder. All rights reserved. No reuse allowed without permission.

endogenous control gene *rpsL* (36) using the ΔCt method. qPCR and qRT-PCR primers and probes are provided in **Table S2**.

Serial passaging experiments on clinical *E. coli* ST131 index bacteremia isolate

p4A passaging experiments with antibiotic selection were performed in LB broth under shaking conditions at 37ºC. A single colony from the index strain of patient 4 (p4A) was grown overnight, then diluted 1:100 into fresh LB containing ertapenem (ETP) (Sigma-Aldrich) at 0.5 MIC ETP. The process was repeated with increasing concentrations of ETP until growth was observed at an ETP concentration of 32 µg/mL. Passaging experiments were performed twice with growth occurring at an ETP MIC of ≥ 32 µg/mL within 3 passages (i.e. 72 hours) on each occasion. For the first passaging experiment, cells were collected on four consecutive days (strains p4A_1 to p4A_4) while continuing to passage at an ETP concentration of 32 µg/mL. This was done in order to determine whether progressive β-lactamase encoding gene amplification would be observed. On the second set of passaging experiments, cells were collected on the first day that the ETP MIC reached ≥ 32 µg/mL, serially diluted onto agar plates, and two different isolates were studied to assess for heterogeneity (strains p4A_H1 and p4A_H2). Additional serial passaging experiments were conducted using p4C and p4D isolates in the absence of antibiotic selection to determine the stability of the amplified units with protocol adapted from previously published methods (37).

β-lactamase cloning and expression analysis

The open reading frames of β-lactamases were amplified from genomic DNA of the *K. pneumoniae* strain MB101 using Q5 polymerase and the primers listed in **Table S2**. Cloned

bioRxiv preprint doi: https://doi.org/10.1101/616961; this version posted March 19, 2020. The copyright holder for this preprint (which was not certified by peer review) is the author/funder. All rights reserved. No reuse allowed without permission.

ORFs were inserted into the arabinose inducible vector pBAD33 by Gibson assembly (38) of purified products. pBAD33$bla_{\text{CTX-M-15}}$ and pBAD33$bla_{\text{OXA-1}}$ were transformed into DH5α *E. coli* and were maintained with 50 μg/mL chloramphenicol in cation adjusted Mueller Hinton (MHII) media. MIC assays were performed with ceftriaxone (Sandoz GmbH), or piperacillin-tazobactam (Fresenius Kabi USA) as follows. DH5α strains carrying pBAD33$bla_{\text{CTX-M-15}}$, pBAD33$bla_{\text{OXA-1}}$, or control vector were grown for 18 hours at 220 rpm at 37°C in MHII with 50 μg/mL chloramphenicol. These cultures were diluted to approximately $5x10^5$ CFU/mL in MHII with 0.2% L-Arabinose or vehicle control, without chloramphenicol. Each strain was exposed to serial dilutions of the above drugs in microtiter plates sealed with gas-permeable membranes (Midsci). Microtiter plates were incubated for 18 hours at 220 rpm at 37°C, followed by OD_{600} measurement in a Biotek Synergy HT plate reader. The lowest tested antibiotic concentration yielding OD_{600} measurement of 0.06 or less in at least two of three replicate wells was considered to be the MIC.

Statistical analyses

All statistical analyses were performed using Stata v13.1 (StataCorp LP, College Station, TX). Bivariate comparisons between patients with recurrent bacteremia and patients with a single bacteremia episode were made with the Wilcoxon Rank-sum test and Fisher's exact test as appropriate based on covariate distributions. Comparisons of DNA and RNA levels among strains was performed using the Kruskall-Wallis test when more than two strains were analyzed or the Wilcoxon Rank-sum test when two strains were analyzed. MIC comparisons were performed using ANOVA with Dunnett's test of multiple comparisons. Statistical significance was assigned as a two-sided P value < 0.05.

bioRxiv preprint doi: https://doi.org/10.1101/616961; this version posted March 19, 2020. The copyright holder for this preprint (which was not certified by peer review) is the author/funder. All rights reserved. No reuse allowed without permission.

279

280 **Data availability**

281 The index isolate assemblies from recurrent bacteremia patients that developed non-CP-CRE as
282 well as the long-read and short-read data for all isolates have been deposited in the National
283 Center for Biotechnology (NCBI) BioProject database PRJNA603908. ONT-sequencing data of
284 non-CP-CRE isolates from a previous study (18) were deposited in NCBI BioProject database
285 PRJNA388450. All other data analyzed during this study are available in the supplemental
286 materials and/or available upon request from the corresponding author.

287

288 **RESULTS**

289 **116 patients with ESBL-E bacteremia were identified from the University of Texas MD**
290 **Anderson Cancer Center (MDACC) from January 2015 to July 2016**

291 Clinical and demographic features are presented on **Table S3**. *E. coli* was the most common
292 organism isolated (100/116; 86.2%), followed by *K. pneumoniae* (14/116; 12.1%), and *K.*
293 *oxytoca* (2/116; 1.7%). Carbapenems were used as primary treatment in 92% of index cases.
294 Recurrent bacteremia was identified in 16/116 (13.8%) patients and primarily occurred either in
295 patients with leukemia or recipients of hematopoietic stem cell transplants (14/16 cases, **Table**
296 **S3**). The majority (14/16) of recurrent bacteremia cases had *E. coli* isolated, with the remaining
297 two cases being due to *K. pneumoniae* infections. Carbapenem-resistant isolates were present in
298 4/16 (25%) recurrent bacteremia patients (**Fig. 1**). All four recurrent isolates that developed
299 carbapenem resistance were *E. coli* isolates from leukemia patients. The full set of serial isolates
300 was available for 11/16 (68.8%) patients, including all strains from the four patients that had at
301 least one recurrent isolate that developed a carbapenem resistant phenotype.

bioRxiv preprint doi: https://doi.org/10.1101/616961; this version posted March 19, 2020. The copyright holder for this preprint (which was not certified by peer review) is the author/funder. All rights reserved. No reuse allowed without permission.

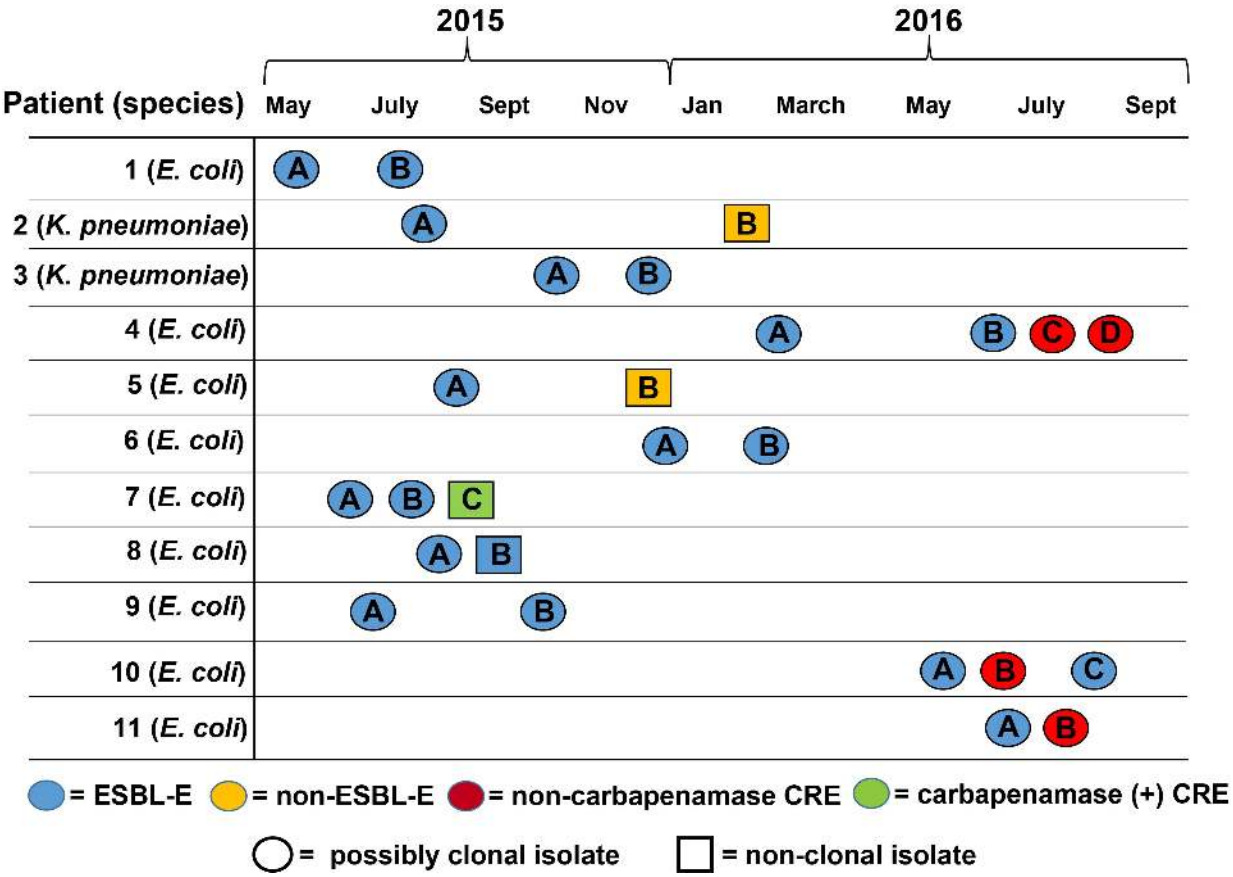

FIG 1 Overview of strains using Illumina short-read data. Timeline showing date of serial isolation from blood cultures. Patient numbers are in the first column. The shape and color of the isolates as labelled in the legend indicate clonality and antimicrobial resistance respectively. Strains were considered possibly clonal if they were the same sequence type and clustered on the phylogenetic tree. Patient subgroups (e.g. Patient 1; isolate A and B) refers to the order of isolation. Abbreviations are as follows: ESBL-E = extended spectrum β-lactamase producing *Enterobacterales*, CRE = carbapenem resistant *Enterobacterales*.

bioRxiv preprint doi: https://doi.org/10.1101/616961; this version posted March 19, 2020. The copyright holder for this preprint (which was not certified by peer review) is the author/funder. All rights reserved. No reuse allowed without permission.

Detection of non-CP-CRE emergence from three sets of clonal, ESBL-E recurrent bacteremia isolates

The 11 sets of patient serial isolates included nine *E. coli* serial isolates and two *K. pneumoniae* serial isolates. We performed Illumina short-read sequencing on the 26 strains identified from the 11 sets of serial isolates. Strain details are provided in **Table S4**. Serial strain relatedness was assessed using phylogenetic analysis with strains considered possibly clonal if they were the same sequence type, had the same Bayesian population structure, and clustered together on the phylogenetic tree (**Fig. S1**). The temporal collection, antimicrobial resistance, and strain relatedness are depicted in **Fig. 1**. Only a single strain, the 3rd isolate from patient 7, which we will abbreviate as p7C, had a carbapenemase based on a positive Neo-Rapid CARB Kit Test result (**Fig. 1**). Whole genome, short-read sequencing analysis confirmed the presence of the class D carbapenemase, *bla*$_{\text{OXA-181}}$ in p7C. Furthermore, p7C was a different sequence type from the patient 7 index strain (p7A) indicating new strain acquisition.

We focused our subsequent analyses on the isolates from patient 4 (p4), patient 10 (p10), and patient 11 (p11), as each had at least one carbapenem resistant recurring non-CP-CRE isolate. Our HiSeq WGS data indicated that all three patients had recurrent *E. coli* isolates that respectively clustered together within a core genome phylogenetic tree, had the same Bayesian hierarchical population structure, and belonged to the same sequence type (**Fig. S1**). We confirmed clonality by measuring pairwise SNP distances between each recurrent isolate and their respective index strain using their highly resolved, ONT consensus assemblies. Our analysis indicated that there were less than 20 SNPs for all respective recurrent strains relative to their

bioRxiv preprint doi: https://doi.org/10.1101/616961; this version posted March 19, 2020. The copyright holder for this preprint (which was not certified by peer review) is the author/funder. All rights reserved. No reuse allowed without permission.

334 index strain suggesting that these three patients had clonal, re-infecting strains that had

335 developed carbapenem resistance through a non-carbapenemase mechanism (**Table 1**).

336

337

Table 1. Clonality, Antibiotic Minimum Inhibitory Concentration (MIC), Outer Membrane Protein, and β-lactamase Characterization of *Enterobacterales* Isolates

Patient	Isolate	ST	Species	Pairwise SNP Distance	CAZ MIC[a]	CEP MIC[a]	TZP MIC[a]	ETP MIC[a]	MEM MIC[a]	*ompC*[b,d]	*ompF*[c,d]	ESBL Amplification
patient 4	p4A	131	*E. coli*	Ref	16	≥64	8	≤0.5	≤0.25	WT	WT	None
	p4B	131	*E. coli*	2	16	8	≥128	≤0.5	≤0.25	WT	WT	$bla_{\text{OXA-1}}$
	p4C	131	*E. coli*	14	16	64	≥128	≥32	4	c.504_505ins[e]	c.548delA	$bla_{\text{OXA-1}}$
	p4D	131	*E. coli*	15	≥64	≥64	≥128	≥32	4	c.504_505ins[e]	c.548delA	$bla_{\text{OXA-1}}$
patient 10	p10A	10	*E. coli*	Ref	16	2	8	≤0.5	≤0.25	WT	WT	None
	p10B	10	*E. coli*	1	≥64	≥64	≥128	≥32	8	c.634_649del	c.77_87del	$bla_{\text{CTX-M-55}}$
	p10C	10	*E. coli*	0	≥64	≥64	16	≤0.5	≤0.25	WT	WT	$bla_{\text{CTX-M-55}}$
patient 11	p11A	131	*E. coli*	Ref	≥64	≥64	64	≤0.5	≤0.5	c.508_521delins[f]	c.305_312del	$bla_{\text{OXA-1}}$, $bla_{\text{CTX-M-15}}$
	p11B	131	*E. coli*	0	≥64	≥64	≥128	4	1	c.508_518del	c.305_312del	$bla_{\text{OXA-1}}$, $bla_{\text{CTX-M-15}}$
NA	MB101	37	*K. pneumoniae*	NA	≥64	≥64	≥128	≥32	8	c.607_626ins[e]	NA	$bla_{\text{OXA-1}}$, $bla_{\text{CTX-M-15}}$
NA	MB746	405	*E. coli*	NA	64	≥64	≥128	≥32	4	c.131insA	c.760_763ins	$bla_{\text{OXA-1}}$, $bla_{\text{CTX-M-15}}$

338 [a]All minimum inhibitory concentrations (MICs) reported in μg/ml; abbreviations for each antibiotic are as follows: CAZ

339 (ceftazidime), CEP (cefepime), TZP (piperacillin-tazobactam), ETP (ertapenem), MEM (meropenem)

340 [b]Uniprot reference entry names for *ompC* are A0A192C9D6_ECOLX, OMPC_ECOLI, and U9Y7F2_ECOLX for ST131, ST10, and

341 ST405 *E. coli* isolates respectively; MB101 porin is *ompK36* with Uniprot reference entry name A0A0H3H0Y2_KLEPH

342 [c]Uniprot reference entry names for *ompF* are A0A192CJUO_ECOLX, OMPF_ECOLI, and S0Z171_ECOLX for ST131, ST10, and

343 ST405 *E. coli* isolates respectively

344

[d]WT indicates ‘wild type’ coding DNA sequence, ‘ins’ indicates insertion, ‘del’ indicates deletion, and ‘delins’ indicates insertion/deletion; all indel events are frame-shift mutations that leave premature, truncated coding DNA sequences unless otherwise noted.

[e]Insertion of MB1860TU_A with variable number of repeating units

[f]INDEL, Y170_N174delinsKR, creates an in-frame OmpC protein

[e]Insertion of 1X copy of MB101TPU

bioRxiv preprint doi: https://doi.org/10.1101/616961; this version posted March 19, 2020. The copyright holder for this preprint (which was not certified by peer review) is the author/funder. All rights reserved. No reuse allowed without permission.

352

353 **Gene amplification and porin loss associated with emergence of non-CP-CRE**

354 Each of the serial isolates that developed a non-CP-CRE phenotype (p4A-D, p10A-C, and p11A-
355 B) had increased Illumina short-read and ONT long-read coverage depth for β-lactamase
356 encoding genes indicating amplification (**Fig. 2, Table S5 and Table S6**). Specifically, we noted
357 increased coverage depth of *bla*$_{\text{OXA-1}}$ in all p4 recurrent isolates, *bla*$_{\text{CTX-M-55}}$ in p10 recurrent
358 isolates, and *bla*$_{\text{OXA-1}}$and *bla*$_{\text{CTX-M-15}}$ in both the index and recurrent isolate of p11 (**Table 1**). We
359 used qPCR to confirm the increased short-read and long-read coverage depth of our WGS
360 analyses and found that the increased coverage depth corresponded to increased transcript levels
361 of the amplified β-lactamase encoding genes (**Fig. 2**).

362

363 We further characterized outer membrane porin genes with our sequencing data as disruptions of
364 these genes are often correlated with carbapenem resistance. The only consistently identified
365 variation in the non-CP-CRE strains relative to their ESBL-E index strains were mutations that
366 disrupted the ORFs of the porin proteins OmpC and OmpF (**Table 1**). The initial sequencing
367 results indicated that an insertion sequence (IS) as well as nucleotide deletions that resulted in
368 frame-shifts mediated *ompC* gene disruption in isolates that developed non-CP-CRE.
369 Conversely, we consistently found frame-shift inducing deletions in *ompF* genes for both the
370 carbapenem susceptible and resistant isolates (**Table 1**). For p10 isolates, interruption of OmpC
371 and OmpF in the second, non-CP-CRE isolate (p10B) was followed by reversion to the WT
372 OmpC and OmpF genes in the third, carbapenem-susceptible isolate (p10C).

bioRxiv preprint doi: https://doi.org/10.1101/616961; this version posted March 19, 2020. The copyright holder for this preprint (which was not certified by peer review) is the author/funder. All rights reserved. No reuse allowed without permission.

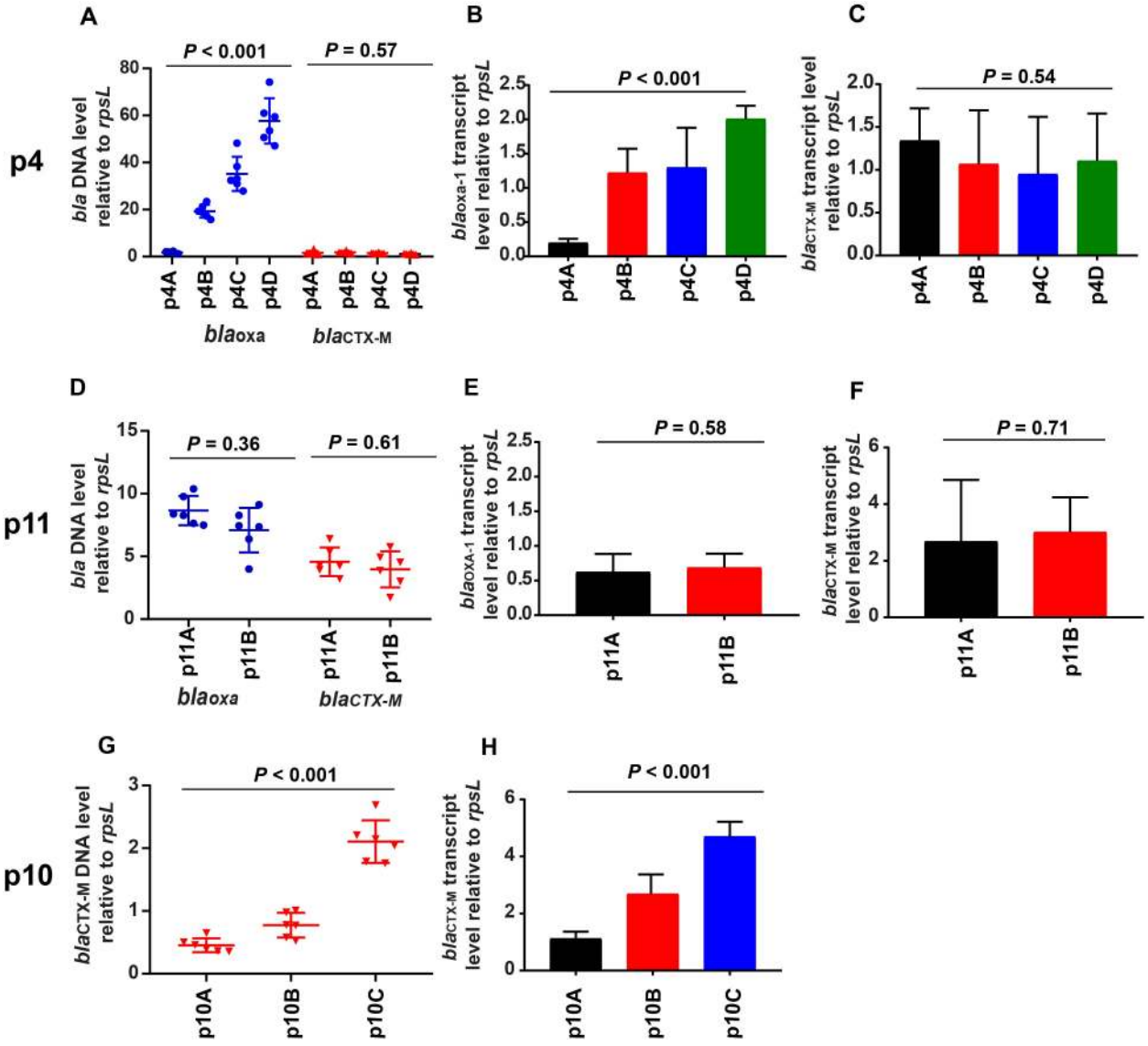

FIG 2 PCR analysis of β-lactamase encoding gene levels and transcript levels. Rows from top to bottom are data from patient 4 (p4), patient 11 (p11), and patient 10 (p10). (A, D, G) Taq-Man qPCR of genomic DNA results collected in triplicate on two separate days (n = 6) for either $bla_{\text{OXA-1}}$ (blue) or $bla_{\text{CTX-M}}$ (red) relative to the endogenous control gene *rpsL*. Data shown are individual data points with mean ± SD superimposed. (B, E, H) $bla_{\text{OXA-1}}$ transcript level relative to endogenous control gene *rpsL*. RNA was collected from mid-exponential phase in triplicate on two separate days (n = 6). Data shown are mean ± SD. (C, F) similar analysis to (B, E, H) except that data are for $bla_{\text{CTX-M}}$. Note that the p10 strains do not contain $bla_{\text{OXA-1}}$. *P* values refer to

bioRxiv preprint doi: https://doi.org/10.1101/616961; this version posted March 19, 2020. The copyright holder for this preprint (which was not certified by peer review) is the author/funder. All rights reserved. No reuse allowed without permission.

382 measurements in the serial isolates relative to initial isolate using the Kruskal-Wallis (p4 and
383 p10) or Wilcoxon rank-sum tests (p11).

384

385 **Class 1 transposon Tn*MB1860* found in both ST131 p4 and p11 serial isolates.**
386 The consensus ONT assembly index strains for patient 4 (p4A) and patient 11 (p11A) both
387 contain an 8,147 bp, IS*26*-mediated translocatable unit (TU), designated as MB1860TU_A,
388 which carries *bla*$_{\text{OXA-1}}$, and inserts upstream adjacent to another 3,985 bp TU, designated
389 MB1860TU_B, that carries *bla*$_{\text{CTX-M-15}}$ (**Fig. 3A**). MB1860TU_C is the combination of both
390 respective TUs that is 12,132 bp in length. The entire putative class 1 transposon structure
391 designated Tn*MB1860* is 12,952 bp (**Fig. 3A**).

392

393 When moving from the 5' to 3' end of Tn*MB1860* using the p4A chromosome (**Fig. 3A;**
394 GenBank Accession #: CP049085) as the reference, the first resistance island contains two
395 flanking IS*26 tnpA* genes in opposite orientation with the aminoglycoside N6'-acetyltransferase
396 variant gene (*aac(6')-Ib-cr*), the oxacillinase gene (*bla*$_{\text{OXA-1}}$), and a truncated chloramphenicol
397 resistance determinant (*ΔcatB3*). Following the second IS*26* element in Tn*MB1860*, there is an
398 aminoglycoside N3'-acetyltransferase III variant gene, *aacC3,* and the tunicamycin resistance
399 gene, *tmrB*. Downstream of the *tmrB* gene is an IS*3* element, which has a modified left inverted
400 repeat (IR_L) and a frame-shifted transposase that has been truncated by a third IS*26* element at
401 the 3' end of the IS*3* transposase. Immediately downstream of this IS*26* element is a truncated
402 Tn2-like transposase which marks the 3' boundary of MB1860TU_A. MB1860TU_A is inserted
403 adjacent to the smaller translocatable unit, MB1860TU_B, which includes another fragment of a
404 Tn2-like transposase, as well as *orf477*, *bla*$_{\text{CTX-M-15}}$, and an IS*Ecp1* truncated by an intact IS*26*,

bioRxiv preprint doi: https://doi.org/10.1101/616961; this version posted March 19, 2020. The copyright holder for this preprint (which was not certified by peer review) is the author/funder. All rights reserved. No reuse allowed without permission.

405 which marks the 3' boundary of both MB1860TU_B, as well as serves as the 3' flanking IS*26*
406 element for the full length Tn*MB1860*. Similar IS*26*/Tn2 family transposable elements that have
407 putatively formed via homologous recombination events have previously been reported in
408 association with IS*26*-mediated AMR transfer in *Enterobacterales* (6, 39, 40).
409
410 Tn*MB1860* is located on the p4 chromosome (1,764,660 – 1,777,611 bp; GenBank Accession #:
411 CP049085) and the p11 chromosome (1,812,524 – 1,825,475 bp; GenBank Accession #:
412 CP049077). One of the signatures of transposition are variable sized direct repeats called target
413 site duplications (TSDs) that flank insertion sequences and are created during the transposition
414 process (41-43). The Tn*MB1860* composite transposon on the p11A chromosome has 7-bp TSDs
415 that indicate a transposition within a 3,762 bp ORF that putatively is involved in molybdopterin
416 cofactor biosynthesis (**Fig. S2**). Interestingly, p4A differs in chromosomal context relative to
417 p11A due to an intramolecular transposition event that occurred in reverse orientation (**Fig. S3)**.
418 This is evidenced by the fact that p4A has an approximately 61 kbp region that is inverted with a
419 downstream IS*26* in inverse orientation that has an 8-bp TSD within the colicin I receptor gene,
420 *cirA*, in reverse complement orientation (**Fig. S3**). An alignment of p4A and p11A with two
421 other *E. coli* ST131 chromosomes, TO217 (GenBank Accession #: LS992192.1) and
422 Ecol_AZ146 (GenBank Accession #: CP018991.1) indicate similar chromosomal carriage of
423 Tn*MB1860* with the noted inversion event that has occurred in the p4A isolate (**Fig. S3**).
424

bioRxiv preprint doi: https://doi.org/10.1101/616961; this version posted March 19, 2020. The copyright holder for this preprint (which was not certified by peer review) is the author/funder. All rights reserved. No reuse allowed without permission.

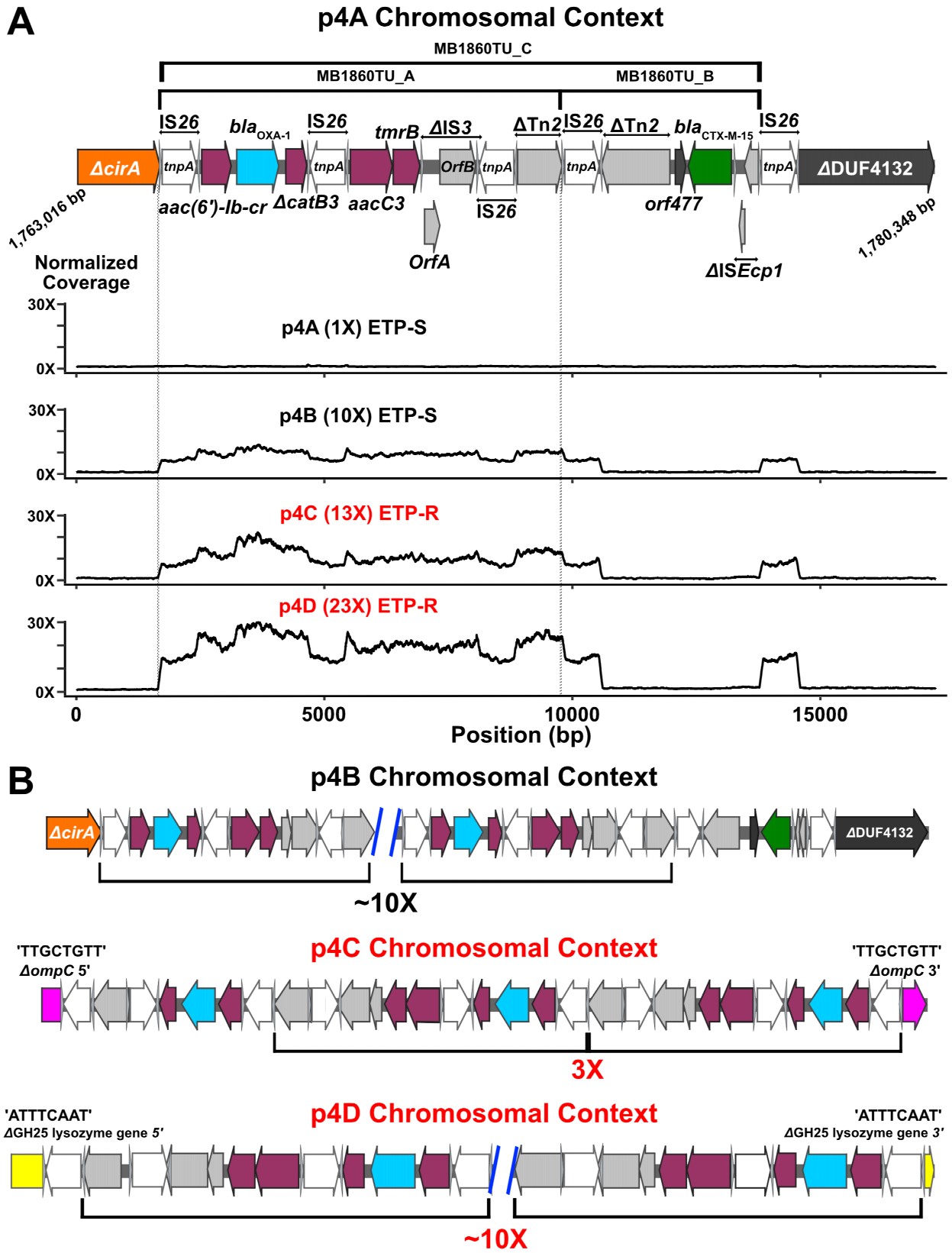

425

bioRxiv preprint doi: https://doi.org/10.1101/616961; this version posted March 19, 2020. The copyright holder for this preprint (which was not certified by peer review) is the author/funder. All rights reserved. No reuse allowed without permission.

426 **FIG 3** Characterization of IS*26*-flanked composite transposon with amplification and
427 transposition of modular translocatable units in patient 4 serial isolates (i.e., p4A – p4D).
428 Terminal left and right inverted repeats (IR_L and IR_R respectively) of insertion sequences (ISs)
429 are specified by grey triangles that bracket respective complete and incomplete *tnpA* genes.
430 ORFs are colored as follows: non-β-lactam AMR encoding genes (maroon), bla_{OXA-1} (blue),
431 $bla_{CTX-M-15}$ (green), IS*26 tnpA* (white), and other IS/Tn elements (gray). (A) Schematic indicates
432 chromosomal context (1,763,016 – 1,780,348 bp; GenBank Accession #: CP049085)) of
433 Tn*MB1860* locus flanked by directly oriented IS*26* transposases found in p4A isolate.
434 Immediately below schematic are normalized, short-read coverage depth line graphs for the four
435 p4 serial isolates with MB1860TU_A bracketed by dotted lines. 'ETP-S' = ertapenem
436 susceptible; 'ETP-R' = ertapenem resistant. Font color for each serial isolate labelled in
437 normalized coverage graph representing carbapenem susceptibility (black) or carbapenem
438 resistance (red). (B) Characterization of amplification, transposition, and ORF disruption events
439 in each of the respective patient 4 recurrent episode isolates. Black brackets beneath ORFs
440 indicate MB168TU_A. The p4B chromosomal context shows a ~10X MB1860TU_A
441 amplification event in the original p4A locus. The p4C chromosomal context additionally
442 contains transposition and disruption of the *ompC* porin gene (pink) ~63 kbp upstream of
443 original p4A *TnMB1860* locus with subsequent amplification. p4D isolate has previous
444 amplification and transposition events found in p4B and p4C as well as another MB1860TU_A
445 transposition and disruption of a putative glycoside hydrolase gene (i.e. GH25; yellow) ~71 kbp
446 downstream of Tn*MB1860* locus with an amplification. The target site duplications (TSDs)
447 created by the transposition of the TU are indicated above each respective junction site that flank
448 the insertion and disruption of the OmpC and GH25 genes respectively.
449

bioRxiv preprint doi: https://doi.org/10.1101/616961; this version posted March 19, 2020. The copyright holder for this preprint (which was not certified by peer review) is the author/funder. All rights reserved. No reuse allowed without permission.

Delineation of MB1860TU_A amplification and transposition in ST131 p4 and p11 serial isolates

Patient 11 isolates p11A and p11B had relatively the same increase in mapping coverage for both *bla*$_{\text{OXA-1}}$ and *bla*$_{\text{CTX-M-15}}$ (**Table S3**). The consensus assemblies of both p11 isolates revealed that this increase in relative short-read coverage was due to two copies of *bla*$_{\text{OXA-1}}$ and *bla*$_{\text{CTX-M-15}}$ being present on a chromosomally located Tn*MB1860* as well as on IS*26*-mediated genomic resistant modules present on a 180,963bp multireplicon, F-type plasmid, p11A_p2 (**Fig. S2, Fig. S3;** GenBank Accession #: CP049079). The CRE phenotype of p11B relative to p11A appears to be driven by additional inactivation of the *ompC* gene given that the *ompF* gene is truncated in both strains (**Table 1**).

In contrast to the p11 isolates, the amplification and transposition of the modular, translocatable units that compose Tn*MB1860* in p4 was completely in a chromosomal context (**Fig. 3**). There was a consistent increase in short-read coverage depth (**Fig. 3A**) of the entire MB1860TU_A structure up to approximately 23-fold in p4D relative to the seven housekeeping pubMLST genes for ST131. We first analyzed strain p4B, which had developed resistance to piperacillin-tazobactam (TZP) but remained carbapenem susceptible (**Table 1**). In p4B, MB1860TU_A generated a ~10X tandem array *in situ* most likely through a conservative, IS*26*-mediated transposition mechanism or homologous recombination (**Fig. 3B**) (44, 45). We were unable to assemble the full-length tandem array due to limitations in read length size. However, we were able to use the SVAnts tool to identify thirty individual reads with two or greater number of tandem arrays of MB1860TU_A with 7 individual reads having 4X copies of *bla*$_{\text{OXA-1}}$. The occurrence of the 10X TU amplification at the original Tn*MB1860* locus was confirmed by

bioRxiv preprint doi: https://doi.org/10.1101/616961; this version posted March 19, 2020. The copyright holder for this preprint (which was not certified by peer review) is the author/funder. All rights reserved. No reuse allowed without permission.

aligning the p4B long-reads to the reference chromosome p4A using SVAnts in conjunction with a short-read pileup analysis. Additionally, all outer membrane protein genes were WT and remained intact with p4B. Given that p4B had developed resistance to TZP relative to p4A (**Table 1**), we sought to determine whether overexpression of *bla*$_{\text{OXA-1}}$ could drive TZP resistance. Inducing *bla*$_{\text{OXA-1}}$ expression through cloning under an arabinose responsive promoter increased TZP MIC 6.8-fold relative to uninduced cells (**Fig. S4**).

Next, we examined the non-CP-CRE serial strains p4C and p4D. Interestingly, in both p4C and p4D a transposition and insertion of MB1860TU_A into *ompC* was present approximately 63 kbp upstream of the original *Tn*MB1860 chromosomal locus (**Fig. 3B**). This *ompC* gene disruption was confirmed through the identification of multiple p4C long-reads > 30 kbp that covered the full transposition site as well as identifying this insertion on the p4C and p4D incomplete chromosomal assemblies. We found two individual long reads that were able to span the full length of the MB1860TU_A array (3X copies) which disrupts *ompC* for p4C and confirmed the exact MB1860TU insertion location within *ompC* (c.504_505ins; **Table 1**). We also were able to identify 8-bp TSDs (‘5-TTGCTGTT-3’) at each end of the *ompC* insertion sites, which indicates MB1860TU_A replicative transposition. The p4D assembly and individual long-reads indicated a second MB1860TU_A transposition and insertion ~67 kbp downstream of the Tn*MB1860* within a GH25 lysozyme gene (**Fig. 3B**). This transposition event could be confirmed by 8-bp TSDs (5’-TTGCTGTT-3’) flanking the full insertion site (**Fig 3B**). A progressive increase in both DNA and RNA levels for *bla*$_{\text{OXA-1}}$ but not *bla*$_{\text{CTX-M-15}}$ in the p4 serial isolates was confirmed using qPCR and qRT-PCR, respectively (**Fig. 2A-C**).

bioRxiv preprint doi: https://doi.org/10.1101/616961; this version posted March 19, 2020. The copyright holder for this preprint (which was not certified by peer review) is the author/funder. All rights reserved. No reuse allowed without permission.

Serial passage of patient 4 index strain with ETP elicits *bla*$_{\text{OXA-1}}$ and *bla*$_{\text{CTX-M-15}}$ amplification through unique translocatable units relative to *in vivo* recurrent strains

We passaged strain p4A in increasing concentration of ertapenem (ETP) to determine whether antimicrobial exposure was driving the genetic changes observed in our serial clinical isolates. Resistance to ETP developed within three passages corresponding to three days, upon which we collected strains for the next four days (p4A_1- p4A_4). Short-read and qPCR analyses demonstrated all four isolates had amplification of both *bla*$_{\text{OXA-1}}$ and *bla*$_{\text{CTX-M-15}}$ relative to the p4A index strain prior to ETP exposure (**Fig 4**). ONT sequencing on all four isolates indicated that similar to p4B, there was *in situ* amplification occurring at the original Tn*MB1680* chromosomal locus. However, the full-length TU, MB1860TU_C, which consists of MB1860TU_A and MB1860TU_B (**Fig 4A**) that harbor *bla*$_{\text{OXA-1}}$ and *bla*$_{\text{CTX-M-15}}$ respectively, was the amplifying structure for the passaged isolates in contrast to what we saw in the *in vivo* isolates where MB1860TU_A was the sole amplifying structure (**Table 2**).

Table 2. p4A Serial Passaging Characterization

Sample	ETP MIC (μg/ml)	*ompC*	*ompF*	*bla*$_{\text{OXA-1}}$ copy #[a]	*bla*$_{\text{CTX-M-15}}$ copy #[a]
p4A_1	≥ 32	c.208T>C; p.Q70X	c.17_18insIS1A	6	7
P4A_2	≥ 32	c.208T>C; p.Q70X	WT	8	9
P4A_3	≥ 32	c.208T>C; p.Q70X	c.62_63insIS1A	6	7
P4A_4	≥32	c.208T>C; p.Q70X	c.517_518insIS1A	6	7
p4A_H1	≥ 32	IS1A variant mediated insertion 96 bp upstream of +1 ompC start site	WT	1	9
p4A_H2	≥ 32	IS1A variant mediated insertion 96 bp upstream of +1 ompC start site	WT	1	17

[a]See Materials and Methods for Calculation

We repeated the experiment and again found that ETP resistance developed within three passages from the p4A isolate. ONT sequencing of the 2nd round of passaged isolates (p4A_H1 and p4A_H2) revealed amplification of MB1860TU_B that harbors *bla*$_{\text{CTX-M-15}}$ solely, which we

bioRxiv preprint doi: https://doi.org/10.1101/616961; this version posted March 19, 2020. The copyright holder for this preprint (which was not certified by peer review) is the author/funder. All rights reserved. No reuse allowed without permission.

514 verified using qPCR (**Fig. 4**). Similar to what we observed *in vivo*, the serially passaged ETP
515 resistant isolates contained inactivating mutations in *ompC* although we did not observe any
516 MB1860TU mediated interruptions (**Table 2**). INDELs inactivating the *ompF* gene were
517 observed in a fraction of the serial isolates suggesting *ompF* inactivation may not be necessary
518 for the development of non-CP-CRE (**Table 2**). We found that p4A responded *in vitro* to ETP
519 similarly to what was observed in our serial clinical isolates by amplification of modular
520 MB1860TU elements with concomitant porin disruption. Nevertheless, there was differential
521 amplification of IS*26* translocatable units demonstrating the modularity of these MGEs.
522
523 In order to determine the chromosomal stability of the MB1860TU tandem arrays in the absence
524 of antibiotic selective pressure, both ertapenem resistant (ETP-R) strains p4C and p4D were
525 passaged for 10 days (~60 generations) without supplemented ertapenem. Both ETP-R recurrent
526 strains consistently maintained carbapenem resistance through 60 generations of growth (**Fig.**
527 **S5**). The p4C and p4D strains had relative copy number decreases of $bla_{\text{OXA-1}}$ from 33 to 18X
528 (45% decrease) and 53 to 42X (21% decrease) respectively (**Fig. S5**). These results indicate that
529 both adapted strains can have persisting carbapenem resistance with associated tandem arrays of
530 amplified $bla_{\text{OXA-1}}$ maintained in the absence of antibiotic exposure.
531

bioRxiv preprint doi: https://doi.org/10.1101/616961; this version posted March 19, 2020. The copyright holder for this preprint (which was not certified by peer review) is the author/funder. All rights reserved. No reuse allowed without permission.

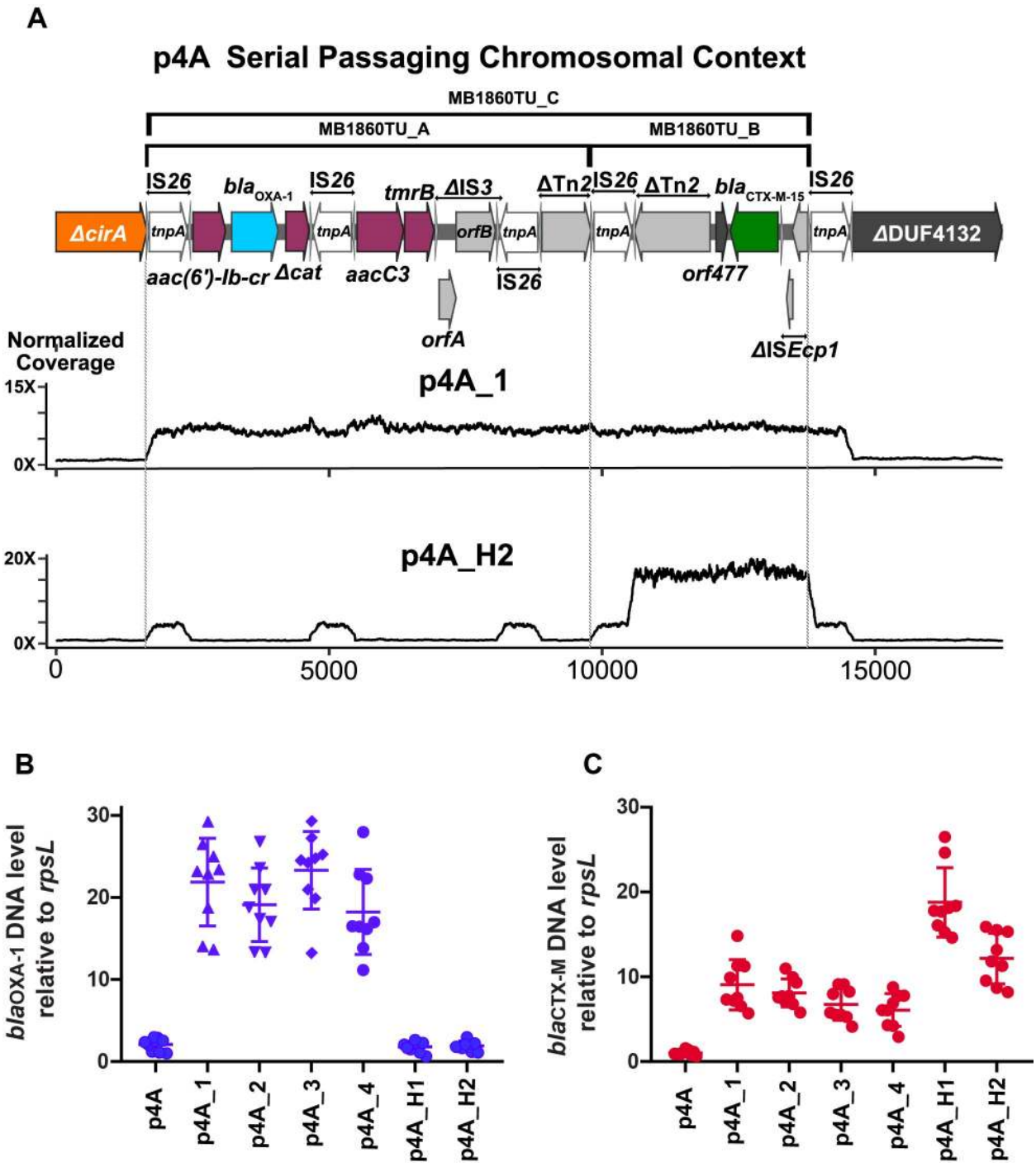

532

533 **FIG 4** Identification and characterization of β-lactamase gene amplification following p4A serial

534 passaging under ertapenem (ETP) exposure. Strain p4A was grown in ETP with isolates p4A_1-

535 4 collected during the 1st round of passaging and p4A_H1 and p4A_H2 collected during the 2nd

536 round. (A) Schematic of Tn*MB1860* locus from p4A as detailed in **FIG 2**. Immediately below

bioRxiv preprint doi: https://doi.org/10.1101/616961; this version posted March 19, 2020. The copyright holder for this preprint (which was not certified by peer review) is the author/funder. All rights reserved. No reuse allowed without permission.

the schematic are normalized, short-read coverage depth line graphs for p4A_1 and p4A_H2 aligned to p4A with location of MB1860TU_A and MB1860TU_B bracketed by dotted lines. Note amplification of MB1860 TU_C in strain p4A_1 whereas only MB1860TU_B amplified in strain p4A_H2. (B) and (C) are Taq-Man qPCR of genomic DNA collected in triplicate on two separate days (n = 6) for either $bla_{\text{OXA-1}}$ (B) or $bla_{\text{CTX-M}}$ (C) relative to the endogenous control gene *rpsL*. Data shown are individual data points with mean ± SD superimposed.

Unique IS*Ecp1*-mediated plasmid transposition of $bla_{\text{CTX-M-55}}$ in patient 10 serial ST10 *E. coli* isolates Compared to the p4 and p11 strains, the serial isolates from patient 10 (p10A – p10C) contain a different MGE that putatively drives the amplification of the ESBL encoding gene, $bla_{\text{CTX-M-55}}$. Index strain p10A harbors $bla_{\text{CTX-M-55}}$ located on an IS*Ecp1* transposition unit designated EC215TPU that resides on a multireplicon FIB-FIC-FII plasmid (**Fig. 5; GenBank Accession #: CP049082**). 'Transposition unit' (TPU) is used here to distinguish from translocatable unit (TU) as they have different transposition mechanisms that are mediated by IS*Ecp1* and IS*26* respectively. There are three additional small plasmids present in p10A, one of which is a ColE1-like 6.8 kbp plasmid designated as p10A_p2 (GenBank Accession #: CP049083), that is highly comparable to pCERC1 (GenBank Accession #: JN012467) (46).

EC215TPU translocates from the multireplicon, type F plasmid in p10A, designated p10A_p1, to p10A_p2 in the second serial isolate p10B (**Fig. 5B**). The IS*Ecp1*-mediated transposition can be identified and confirmed by the 5-bp TSDs that are immediately upstream of the IS*Ecp1* 14 bp IR_L and downstream of another alternative, 14 bp right inverted repeat (IRRalt) respectively (41, 42, 47). There are TSDs flanking EC215TPU at the p10A_p2 recombination site with both the

bioRxiv preprint doi: https://doi.org/10.1101/616961; this version posted March 19, 2020. The copyright holder for this preprint (which was not certified by peer review) is the author/funder. All rights reserved. No reuse allowed without permission.

560 $IR_{:L}$ and IRRalt represented as a blue triangle (5'-CCTCACACCTTCGA-3') on **Fig. 5B**.
561 Notably, as the entire insertion region with three *bla*$_{CTX-M-55}$ copies on p10B has 5 bp TSDs (5'-
562 GATAT-3') that flank IR_L and IR_{Ralt} respectively, one can postulate that an amplification event
563 occurred on p10A_p1, which then subsequently inserted into p10A_p2 (**Fig. 5B)**. p10B is also
564 the only carbapenem-resistant p10 serial isolate. This likely is due in part to deletions in *ompC*
565 and *ompF* that create frame-shift truncations of each respective porin in contrast to the WT
566 genotypes of each respective porin found in p10A and p10C. When analyzing the third isolate
567 p10C, there only is one copy of *bla*$_{CTX-M-55}$ identified in the assembly and short-reads on
568 p10A_p2. However, the short-read and long-read coverage depth analysis suggests an increase in
569 copy number (**Table S6**). The subsequent increase in initiation RNA genes, a marker for ColE1-
570 like plasmids with *bla*$_{CTX-M-55}$ suggests that p10C amplification occurs by an increase in the
571 overall copy number of p10A_p2. These data are consistent with our qPCR analysis which
572 demonstrate progressively higher DNA levels of *bla*$_{CTX-M-55}$ for each serial isolate (**Fig. 2**).
573

bioRxiv preprint doi: https://doi.org/10.1101/616961; this version posted March 19, 2020. The copyright holder for this preprint (which was not certified by peer review) is the author/funder. All rights reserved. No reuse allowed without permission.

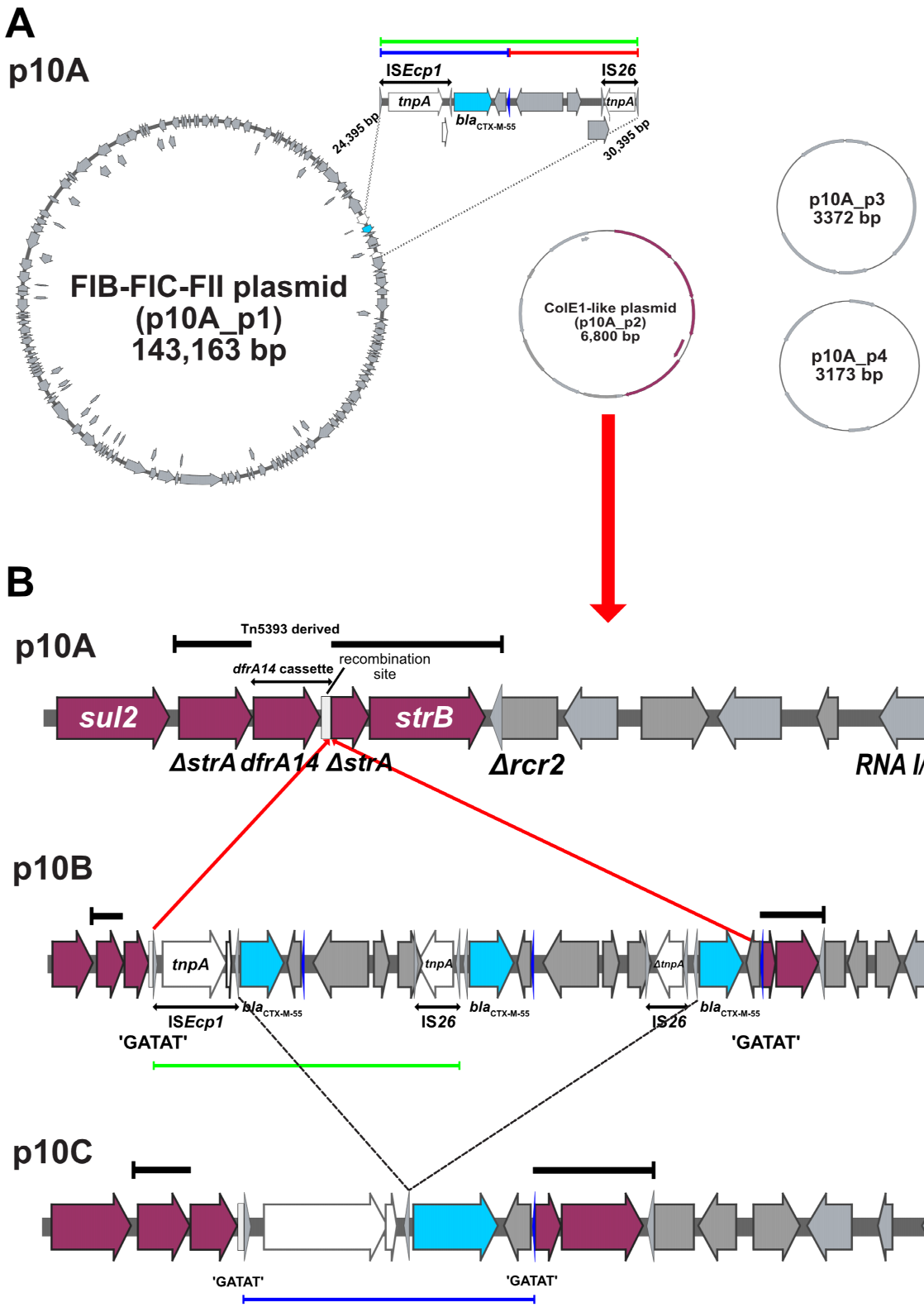

574

bioRxiv preprint doi: https://doi.org/10.1101/616961; this version posted March 19, 2020. The copyright holder for this preprint (which was not certified by peer review) is the author/funder. All rights reserved. No reuse allowed without permission.

FIG 5 Genomic analysis of IS*Ecp1*-mediated mobilization of $bla_{\text{CTX-M-55}}$ from a multireplicon F type plasmid (GenBank Accession #: CP049082) to a ColE1-like, high copy number plasmid (GenBank Accession #: CP049083) in p10 isolates. (A) Non-chromosomal genomic context for patient 10 index strain (p10A) harboring four circular plasmid structures. The $bla_{\text{CTX-M-55}}$ gene is located on a 143,163 bp FIB-FIC-FII plasmid (p10A_p1) on an IS*Ecp1*-$bla_{\text{CTXM-5-55}}$-IS*26* 5945 bp transposition unit (TPU) indicated by a green bracket. The blue and red regions are the union of this green bracketed region and represent regions highlighted in the following section. (B) Progression of TPU insertion into ColE1-like plasmid (p10A_p2). p10A illustrates the full genome context of p10A_p2 including the *sul2-ΔstrA-dfrA14-ΔstrA-strB* resistance island. The top black, bracketed region indicates genome that is derived from the Tn5393 transposon. The region indicated by double-ended arrows indicates where the *dfrA14* cassette inserted itself into Tn5393. The box downstream of *dfrA14* indicates the *attC* recombination site. p10B shows the amplified TPU (11,939 bp) insertion into the p10A_p2 recombination site (indicated by red arrows). The region is bracketed by 5-bp TSDs (5'-GATAT-3') indicative of IS*Ecp1* mediated transposition. An alternative, right inverted repeat (IRRalt) is indicated by blue triangle. p10C contains an 8,998 bp deletion (black dotted lines) where two copies of $bla_{\text{CTX-M-55}}$ are dropped. This creates a TPU flanked by the IRL and IRRalt of IS*Ecp1* (blue bracket).

Detection of β-lactamase gene amplification and porin disruption by AMR elements in non-serial *Enterobacterales* strains

There were two non-CP-CRE strains, MB101 (*K. pneumoniae*) and MB746 (*E. coli*), identified in a previous study examining the role of short-read WGS in predicting β-lactam resistance (**Table 1)** (18). We performed ONT sequencing on the two isolates to determine whether

bioRxiv preprint doi: https://doi.org/10.1101/616961; this version posted March 19, 2020. The copyright holder for this preprint (which was not certified by peer review) is the author/funder. All rights reserved. No reuse allowed without permission.

598 mechanisms of gene amplification and porin disruption were similar to what was observed in the
599 cohort of non-CP-CRE bacteremia serial isolates. Both isolates contain IS*26*-mediated TUs
600 carrying $bla_{\text{OXA-1}}$ as previously characterized in Tn*MB1860* (**Fig. 6**).
601
602 For strain MB101 (**Fig. 6A-B**), a ST37 *K. pneumoniae* isolate, the ~9310 bp IS*26*-mediated TU,
603 designated MB101TU harbors *aac-(6')-Ib-cr,* $bla_{\text{OXA-1}}$, Δ*catB3*, *aacC3,* and *tmrB* and is nearly
604 identical (100% coverage; 99.9% ID) to MB1860TU_A found in serial *E. coli* isolates from
605 patients 4 and 11 (**Fig. 6A**). An IS*Ecp1*-mediated TPU harboring $bla_{\text{CTX-M-15}}$, designated
606 MB101TPU, was also present on the MB101 chromosome as well as an FIB_{K} type plasmid, with
607 at least five copies present on the chromosome based on the Flye assembly and individual long
608 reads. The assembly and long reads indicate the transposition of MB101TPU into a putative
609 glycoporin encoding gene which was followed by the transposition of MB101TU to an existing
610 IS*26* element downstream of MB101TPU (**Fig. 6A**). We identified an amplification of
611 MB101TU at this locus that created a tandem array of at least 8X copies based on the
612 identification of multiple long-reads with multiple MB101TU copies. Interestingly, there was
613 also a transposition event of MB101TPU into the *ompK36* encoding gene, a homolog of *ompC* in
614 *E. coli* (**Fig. 6B**). Thus, MB101 has amplification of both $bla_{\text{OXA-1}}$ and $bla_{\text{CTX-M-15}}$ via distinct
615 mechanisms along with TPU mediated porin disruption.
616
617 The ST405 *E. coli* isolate, MB746, has an IS*26*-mediated translocatable unit, designated
618 MB746TU, which also includes a genomic resistance module that carries *aac(6')-Ib-cr,* $bla_{\text{OXA-1}}$,
619 and a truncated chloramphenicol resistance determinant (**Fig. 6C-D**) similar to what is seen on
620 MB1860TU_A. MB746TU carries an additional tetracycline resistance operon and macrolide

bioRxiv preprint doi: https://doi.org/10.1101/616961; this version posted March 19, 2020. The copyright holder for this preprint (which was not certified by peer review) is the author/funder. All rights reserved. No reuse allowed without permission.

resistance operon, not present on Tn*MB1860*. We found four individual long-reads that carried at least 3X copies of MB746TU present in the same MB746 chromosomal location (**Fig. 6C**). Additionally, we identified a FIB plasmid that harbored both $bla_{\text{OXA-1}}$ and $bla_{\text{CTX-M-15}}$ which has a similar configuration and orientation to Tn*MB1860* (Red bracket; **Fig. 6D**). The IS*26*-mediated TU carrying $bla_{\text{CTX-M-15}}$ has 99.7% BLAST identity with MB1860_B with the only substantial difference being a size of 5558 bp vs the 3985 bp MB1860TU_B (**Fig. 6D**). Notably, MB746 also had *ompC* and *ompF* gene disruptions (**Table 1)** comparable to what was observed in serial isolates that developed non-CP-CRE phenotypes with concomitant β-lactamase amplifications. These data show that there are multiple, non-CP-CRE clinical isolates within our region that have amplification and transposition of similar IS*26* and IS*Ecp1*-mediated elements that harbor β-lactamase genes encoding genes in conjunction with porin disruption.

bioRxiv preprint doi: https://doi.org/10.1101/616961; this version posted March 19, 2020. The copyright holder for this preprint (which was not certified by peer review) is the author/funder. All rights reserved. No reuse allowed without permission.

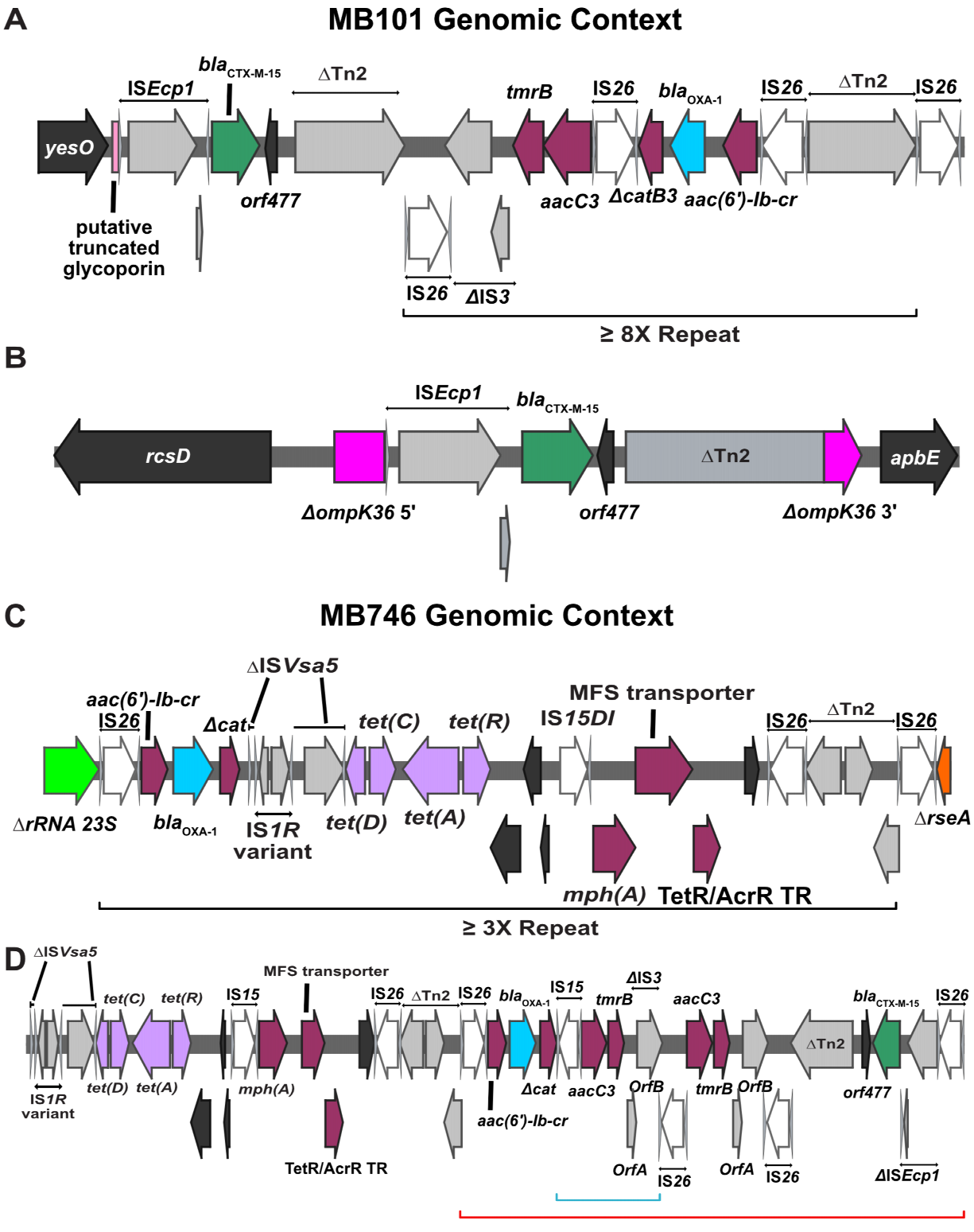

633

634 **FIG 6** Genomic context of end-stage MB101 and MB746 isolates respectively. Terminal left and

635 right inverted repeats (IR_L and IR_R respectively) of insertion sequences (ISs) are specified by

bioRxiv preprint doi: https://doi.org/10.1101/616961; this version posted March 19, 2020. The copyright holder for this preprint (which was not certified by peer review) is the author/funder. All rights reserved. No reuse allowed without permission.

636 grey triangles that bracket respective complete and incomplete *tnpA* genes. ORFs are colored as
637 follows: AMR genes (maroon), *bla*$_{\text{OXA-1}}$ (blue), *bla*$_{\text{CTX-M-15}}$ (green), IS26 *tnpA* (white), and other
638 IS/Tn elements (gray). Delta (Δ) next to annotated genetic region indicates a truncation or
639 disruption (A-B) Chromosomal locations of MB101TU (Fig. 6A) and MB101TPU (Fig. 6B)
640 indicating respective amplification and transposition of each element. ~8X MB101TU repeat
641 indicated by black bracket. Truncated *ompK36* gene labelled in pink (Fig. 6B). (C-D) Genomic
642 context of MB746TU and respective genomic resistance modules carrying AMR genes. Black
643 brackets beneath Fig. 6C schematic indicate repeating MB101TU unit. Fig. 6D indicates FIB
644 plasmid carriage of genomic resistance modules. Red bracket indicates IS*26* transposon structure
645 that shares 100% coverage; 99% BLAST similarity with Tn*MB1860*. Blue bracket indicates
646 small, 2X repeat structure.
647
648 **DISCUSSION**
649 While recent systematic surveillance studies indicate that the prevalence of non-CP-CRE
650 remains high (3, 4), the mechanisms contributing to non-CP-CRE emergence within clinical
651 settings are largely unknown. This public health issue is particularly troublesome given the
652 difficulties in properly diagnosing non-CP-CRE infections and prescribing effective
653 antimicrobials due to the transient nature of their carbapenem resistance phenotypes as well as
654 their lack of a carbapenemase. This analysis demonstrates that multiple TU- and TPU-mediated
655 modular amplifications of β-lactamase encoding genes in conjunction with porin inactivation are
656 driving non-CP-CRE emergence in our cohort of cancer patients with recurrent bacteremia . It is
657 well established that “copy-in” replicative transposition is a common mechanism by which IS*26*-
658 mediated TUs mobilize to regions lacking a pre-existing IS*26* element (43, 45, 48). Recent

bioRxiv preprint doi: https://doi.org/10.1101/616961; this version posted March 19, 2020. The copyright holder for this preprint (which was not certified by peer review) is the author/funder. All rights reserved. No reuse allowed without permission.

659 studies have shown that TUs can create tandem resistance gene arrays by targeting genomes with
660 an existing copy of IS*26* through an intermolecular, conservative transposition mechanism and,
661 less frequently, through RecA-dependent homologous recombination (43-45, 49). We were able
662 to determine that the initial incorporation of the composite transposon Tn*MB1860* as well as
663 MB1860TU_A transposition into *ompC* and the predicted glycoside hydrolase gene occurred
664 through a replicative transposition mechanism based on characteristic TSDs at insertion sites.
665 The amplification of MB1860TU_A, MB1860TU_B, and MB1860TU_C that created tandem
666 arrays of resistance genes observed in our study likely occurred through a conservative
667 transposition mechanism although RecA-dependent homologous recombination could also be
668 contributing to the generation of these tandem arrays. The ability to detect genetic structures
669 capable of amplifying β-lactamase encoding genes that synergistically insert into porin encoding
670 genes will be essential for diagnostic and surveillance purposes in order to ensure we are
671 properly identifying clinical isolates that have the ability to develop CRE.
672
673 Amplification of $bla_{\text{OXA-1}}$ in both serial and non-serial isolates consistently included *aac-(6')-Ib-*
674 *cr* and Δ*catB3* in association with other modular, IS*26*-mediated translocatable units carrying
675 resistance genes. Livermore et al. recently observed the co-occurrence of *aac-(6')-Ib'* and
676 $bla_{\text{OXA-1}}$ in 147/149 *E. coli* strains, primarily ST131 isolates, suggesting that many *E. coli*
677 isolates carrying $bla_{\text{OXA-1}}$ may be capable of this amplification (40, 50). The finding that $bla_{\text{OXA-1}}$
678 amplification was consistently associated with progressive development of β-lactam resistance
679 was somewhat surprising given that this enzyme is typically considered a narrow spectrum β-
680 lactamase (51). However, overexpression of $bla_{\text{OXA-1}}$ using an arabinose inducing promoter was
681 shown to generate resistance to ertapenem in a porin deficient strain (6). This study, along with

bioRxiv preprint doi: https://doi.org/10.1101/616961; this version posted March 19, 2020. The copyright holder for this preprint (which was not certified by peer review) is the author/funder. All rights reserved. No reuse allowed without permission.

682 our own results, indicates that *bla*$_{\text{OXA-1}}$ likely contains sufficient carbapenem hydrolysis activity
683 to generate resistance with the combination of augmented gene copy number and decreased
684 carbapenem concentration due to porin inactivation. Additionally, we demonstrate that
685 overexpression of *bla*$_{\text{OXA-1}}$ without porin inactivation produced TZP resistance, a finding that
686 could help resolve previously noted discrepancies between β-lactamase gene content and TZP
687 susceptibility (18, 52). Similar amplifications of the narrow-spectrum, TEM β-lactamases have
688 also been shown to be associated with TZP resistance, suggesting amplification of narrow-
689 spectrum β-lactamases may be a substantial mechanism contributing to TZP resistance (9-11).
690
691 The other amplified β-lactamase in our cohort was *bla*$_{\text{CTX-M}}$. CTX-M is the most commonly
692 identified ESBL enzyme in *Enterobacterales* (53) and high level CTX-M production has
693 previously been shown to confer carbapenem resistance in porin-deficient *E. coli* (6) as well as
694 *K. pneumoniae* (54). Amplification of MB1860TU_B harboring *bla*$_{\text{CTX-M-15}}$ with concomitant
695 porin disruption was associated with development of ETP resistance in one of our two passaging
696 experiments, demonstrating the versatility of various modules of Tn*MB1860* in responding to
697 carbapenem exposure. Unlike *bla*$_{\text{OXA-1}}$, we did not identify *bla*$_{\text{CTX-M}}$ genes in association with
698 other AMR encoding elements, but rather *bla*$_{\text{CTX-M}}$ genes were consistently present with an
699 IS*ECp1* element, which has been previously described for *E. coli* (55, 56). The array of
700 mechanisms by which *bla*$_{\text{CTX-M}}$ copy numbers could increase included (1) *in situ* IS*26*-mediated
701 amplification of MB1860TU_B (strain P4A_H1) and MB1860TU_C (strain p4A1 – p4A4); (2)
702 IS*Ecp1*-mediated transposition of EC215TPU from a low-copy, F-type plasmid to a multi-copy,
703 ColE1-like plasmid (strain p10B); (3) and multiple chromosomal IS*Ecp1*-mediated transposition
704 unit insertions including into the *ompK36* porin encoding gene (strain MB101). Thus, the various

bioRxiv preprint doi: https://doi.org/10.1101/616961; this version posted March 19, 2020. The copyright holder for this preprint (which was not certified by peer review) is the author/funder. All rights reserved. No reuse allowed without permission.

705 *bla*$_{CTX-M}$ amplification mechanisms suggest that augmentation of *bla*$_{CTX-M}$ copy number may be a
706 major driver of non-CP-CRE development.
707
708 Along with permitting direct visualization of genomic resistance module amplifications
709 containing various β-lactamase genes, ONT sequencing also allowed for identifying porin-
710 mediated disruption by TU and TPU structures. Laboratory studies that generated CRE strains
711 through serial passaging have consistently found that OmpC and OmpF porin production is
712 reduced in carbapenem resistant isolates, but mechanisms have generally involved alterations in
713 the porin regulatory protein OmpR or in OmpR binding sites (6, 7). Similarly, a recent study of a
714 single patient with recurrent *E. coli* infection identified a single amino acid change in OmpR as
715 leading to loss of OmpC and OmpF expression with development of ertapenem resistance (15).
716 Conversely, we observed direct inactivation of OmpC and OmpF either through TU/TPU
717 transposition into their respective ORFs or through INDELs that resulted in frame-shift
718 mutations whereas no alterations in OmpR were identified in our cohort. To our knowledge,
719 there have been only two other reports of an IS*Ecp1*-mediated TPU harboring a β-lactamase
720 encoding gene causing the disruption of a porin, in both cases OmpK35 from *K. pneumoniae* (57,
721 58). While there have been a number of studies that have implicated IS-mediated porin
722 disruptions, including IS*26* mediated disruptions (54, 59-61), to our knowledge, this is the first
723 documented IS*26*-mediated translocatable unit disruption of an outer membrane porin followed
724 by amplification of a β-lactamase gene. Given the length of the TUs, as well as the fact that they
725 have the ability to amplify and create tandem arrays once inserted into the porin encoding genes,
726 it is unlikely that targeted PCR based strategies or commonly used short-read approaches alone
727 would have been able to identify the full extent of the TUs observed in our study. Thus,

bioRxiv preprint doi: https://doi.org/10.1101/616961; this version posted March 19, 2020. The copyright holder for this preprint (which was not certified by peer review) is the author/funder. All rights reserved. No reuse allowed without permission.

728 performing long read sequencing on larger cohorts of *Enterobacterales* with porin deficient
729 backgrounds should reveal whether TU/TPUs harboring AMR genes are a frequent mediator of
730 porin gene disruption, but have not been previously identified due to the long and repetitive
731 nature of the involved DNA structures.
732
733 The clinical impact of β-lactamase gene amplification and porin loss driving carbapenem
734 resistance has been postulated to be mitigated by the fitness costs imposed on the organism by
735 such genetic changes (37, 62-64). However, such AMR mechanisms are increasingly being
736 recognized as commonly occurring in clinical isolates, including in the serious infections
737 described in our cohort (37, 62-64). This would suggest that organisms with the capability to
738 amplify AMR genes are widespread and capable of causing significant human infections
739 especially under antibiotic selective pressure (7, 9, 10, 65). Moreover, the most recent systematic
740 data on CRE in the U.S. found no difference in outcomes between patients with CRE and non-
741 CP-CRE suggesting that circulating non-CP-CRE organisms may not have significant fitness
742 defects (4). Furthermore, our own results from serial passaging p4C and p4D without ETP
743 exposure suggests these amplified structures harboring AMR genes associated with increased
744 MICs to ertapenem and meropenem may be fairly stable in the absence of antibiotic selective
745 pressure. The chromosomal context of Tn*MB1860* may provide insights into the stability of this
746 structure as a previous study had noted stable transposon carriage when mobilized from plasmid
747 to chromosome at very low levels of antibiotic exposure (66).
748
749 In addition to possibly imposing a fitness cost on the organism, AMR gene amplifications have
750 also been associated with the presence of antimicrobial heteroresistance (65, 67). The interplay

bioRxiv preprint doi: https://doi.org/10.1101/616961; this version posted March 19, 2020. The copyright holder for this preprint (which was not certified by peer review) is the author/funder. All rights reserved. No reuse allowed without permission.

751 between AMR gene amplification, heteroresistance and fitness is likely reflected in the genotype
752 changes of patient 10 isolates given the development and subsequent reversion of porin
753 mutations observed in those strains (Table 1). Recent systematic surveys have indicated
754 approximately 25% of strains reported as carbapenem resistant tested as susceptible at a central
755 laboratory, likely reflecting the transient phenomenon of AMR heteroresistance (4, 64). A
756 limitation of our study is that we only sequenced a single colony for each isolate, which almost
757 certainly underestimates the genetic complexity of a bacterial population responding to
758 antimicrobial therapy. Nevertheless, a challenge presents itself in capturing population
759 heterogeneity with a single genome assembly as multiple, heterogeneous sequencing reads will
760 break current assembler algorithms.
761

762 **CONCLUSIONS**

763 We have used serial, clinical isolates subjected to complementary WGS approaches to identify
764 that a combination of porin inactivation and IS-mediated amplification of TU and TPU elements
765 harboring β-lactamase encoding genes underlies the emergence of non-CP-CRE from ESBL-E
766 parental isolates within our study population. We predict that more widespread application of
767 long-read sequencing technologies will facilitate appreciation of the mechanisms and impact of
768 TU- and TPU-mediated transpositions, porin disruptions, and gene amplifications on a diverse
769 array of AMR pathogens in the clinical setting.
770

771 **LIST OF ABBREVIATIONS**

772 non-carbapenemase-producing carbapenem resistant *Enterobacterales* = non-CP-CRE;
773 translocatable unit = TU; transposition unit = TPU

bioRxiv preprint doi: https://doi.org/10.1101/616961; this version posted March 19, 2020. The copyright holder for this preprint (which was not certified by peer review) is the author/funder. All rights reserved. No reuse allowed without permission.

774

775 **DECLARATIONS**

776 **Ethics approval and consent to participate:** A waiver of informed consent to collect clinical
777 data from electronic medical records and analyze the isolates was provided by the MDACC IRB
778 (PA15-0799). A waiver of consent from UTHealth Science Center at Houston (IRB #: HSC-
779 SPH-20-0032) was obtained to perform bacterial genomics sequencing and analysis.

780

781 **Consent for publication:** Not applicable

782

783 **Availability of data and materials:** The index isolate assemblies from recurrent bacteremia
784 patients that developed non-CP-CRE as well as the long-read and short-read data for all isolates
785 have been deposited in the National Center for Biotechnology (NCBI) BioProject database
786 PRJNA603908. ONT-sequencing data of non-CP-CRE isolates from a previous study (18) were
787 deposited in NCBI BioProject database PRJNA388450. All other data analyzed during this study
788 are available in the supplemental materials and/or available upon request from the corresponding
789 author.

790

791 **Competing interests**: The authors declare that they have no competing interests

792

793 **Funding**: Financial support for this study was provided by the Shelby Foundation (R. Lee Clark
794 Fellow Award to SAS). Sequencing was performed at the MDACC DNA sequencing facility
795 which is supported by the National Cancer Institute [grant number P30-CA016672 via the
796 Bioinformatics Shared Resource].

bioRxiv preprint doi: https://doi.org/10.1101/616961; this version posted March 19, 2020. The copyright holder for this preprint (which was not certified by peer review) is the author/funder. All rights reserved. No reuse allowed without permission.

JK is supported by the Cancer Prevention and Research Institute of Texas (RP150596). Other support provided by the UT Southwestern DocStars award (DEG, JK). JGP is supported by the NIAID (1K01AI143881-01). CAA is supported by NIH/NIAID grants K24AI121296, R01AI134637, R21AI143229, UTHealth Presidential Award, University of Texas System STARS Award, and Texas Medical Center Health Policy Institute Funding Program.

Author contributions: WCS developed the database, generated and analyzed the data, and was a major contributor to the writing of the manuscript. SLA designed the study, collected and analyzed the data, and significant contributor to writing the manuscript. RP helped designed the study, performed the experiments, and analyzed the data. JK performed experiments and analyzed the data. MB performed the experiments and contributed to writing the paper. XL helped perform phylogenomic analyses. AK helped perform phylogenomic analyses and contributed to writing the paper. JGP contributed to the design of the study, analyzed the isolates, and writing of the paper. PS collected and curated the isolates. CAA helped design the study, analyze the data, and writing of the paper. DEG analyzed the data and contributed to the writing of the paper. BMH wrote scripts to analyze the data, analyzed the data, and contributed to writing the paper. SAS designed the study, analyzed the data, and major contributor to the writing of the manuscript. All authors read and approved the final manuscript.

Acknowledgements: We thank the personnel of the clinical microbiology laboratory at MD Anderson Cancer Center for assistance with collecting isolates. Would also like to thank Jennifer Walker, PhD for her insightful input in drafting the manuscript.

bioRxiv preprint doi: https://doi.org/10.1101/616961; this version posted March 19, 2020. The copyright holder for this preprint (which was not certified by peer review) is the author/funder. All rights reserved. No reuse allowed without permission.

REFERENCES

1. CDC. Antibiotic Resistance Threats in the United States, 2019. Atlanta, GA: U.S. Department of Health and Human Services, CDC; 2019.
2. Logan LK, Weinstein RA. The Epidemiology of Carbapenem-Resistant Enterobacteriaceae: The Impact and Evolution of a Global Menace. J Infect Dis. 2017;215(suppl_1):S28-S36.
3. Guh AY, Bulens SN, Mu Y, Jacob JT, Reno J, Scott J, et al. Epidemiology of Carbapenem-Resistant Enterobacteriaceae in 7 US Communities, 2012-2013. JAMA. 2015;314(14):1479-87.
4. Duin Dv, Arias C, Komarow L, Chen L, Hanson B, Weston G, et al. Molecular and Clinical Epidemiology of Carbapenem-Resistant Enterobacteriaceae in the United States: a Prospective Cohort Study. Lancet ID. 2020.
5. Tangden T, Adler M, Cars O, Sandegren L, Lowdin E. Frequent emergence of porin-deficient subpopulations with reduced carbapenem susceptibility in ESBL-producing Escherichia coli during exposure to ertapenem in an in vitro pharmacokinetic model. J Antimicrob Chemother. 2013;68(6):1319-26.
6. Adler M, Anjum M, Andersson DI, Sandegren L. Influence of acquired beta-lactamases on the evolution of spontaneous carbapenem resistance in Escherichia coli. J Antimicrob Chemother. 2013;68(1):51-9.
7. van Boxtel R, Wattel, A. A., Arenas, J., Goessens, W. H., & Tommassen, J. Acquisition of Carbapenem Resistance by Plasmid-Encoded-AmpC-Expressing Escherichia coli. Antimicrobial agents and chemotherapy. 2017;61(1):e01413-16.
8. Beceiro A, Maharjan S, Gaulton T, Doumith M, Soares NC, Dhanji H, et al. False extended-spectrum {beta}-lactamase phenotype in clinical isolates of Escherichia coli associated with increased expression of OXA-1 or TEM-1 penicillinases and loss of porins. J Antimicrob Chemother. 2011;66(9):2006-10.
9. Schechter LM, Creely DP, Garner CD, Shortridge D, Nguyen H, Chen L, et al. Extensive Gene Amplification as a Mechanism for Piperacillin-Tazobactam Resistance in Escherichia coli. MBio. 2018;9(2).
10. Rodriguez-Villodres A, Gil-Marques ML, Alvarez-Marin R, Bonnin RA, Pachon-Ibanez ME, Aguilar-Guisado M, et al. Extended-spectrum resistance to beta-lactams/beta-lactamase inhibitors (ESRI) evolved from low-level resistant Escherichia coli. J Antimicrob Chemother. 2019.
11. Hansen KH, Andreasen MR, Pedersen MS, Westh H, Jelsbak L, Schonning K. Resistance to piperacillin/tazobactam in Escherichia coli resulting from extensive IS26-associated gene amplification of blaTEM-1. J Antimicrob Chemother. 2019;74(11):3179-83.
12. Poirel L, Heritier C, Spicq C, Nordmann P. In vivo acquisition of high-level resistance to imipenem in Escherichia coli. J Clin Microbiol. 2004;42(8):3831-3.
13. Oteo J, Delgado-Iribarren A, Vega D, Bautista V, Rodriguez MC, Velasco M, et al. Emergence of imipenem resistance in clinical Escherichia coli during therapy. Int J Antimicrob Agents. 2008;32(6):534-7.

bioRxiv preprint doi: https://doi.org/10.1101/616961; this version posted March 19, 2020. The copyright holder for this preprint (which was not certified by peer review) is the author/funder. All rights reserved. No reuse allowed without permission.

14. Chia JH, Siu LK, Su LH, Lin HS, Kuo AJ, Lee MH, et al. Emergence of carbapenem-resistant Escherichia coli in Taiwan: resistance due to combined CMY-2 production and porin deficiency. J Chemother. 2009;21(6):621-6.
15. Dupont H, Choinier P, Roche D, Adiba S, Sookdeb M, Branger C, et al. Structural Alteration of OmpR as a Source of Ertapenem Resistance in a CTX-M-15-Producing Escherichia coli O25b:H4 Sequence Type 131 Clinical Isolate. Antimicrob Agents Ch. 2017;61(5).
16. Kao CY, Chen JW, Liu TL, Yan JJ, Wu JJ. Comparative Genomics of Escherichia coli Sequence Type 219 Clones From the Same Patient: Evolution of the IncI1 blaCMY-Carrying Plasmid in Vivo. Front Microbiol. 2018;9:1518.
17. Zou H, Xiong SJ, Lin QX, Wu ML, Niu SQ, Huang SF. CP-CRE/non-CP-CRE Stratification And CRE Resistance Mechanism Determination Help In Better Managing CRE Bacteremia Using Ceftazidime-Avibactam And Aztreonam-Avibactam. Infect Drug Resist. 2019;12:3017-27.
18. Shelburne SA, Kim J, Munita JM, Sahasrabhojane P, Shields RK, Press EG, et al. Whole-Genome Sequencing Accurately Identifies Resistance to Extended-Spectrum beta-Lactams for Major Gram-Negative Bacterial Pathogens. Clin Infect Dis. 2017;65(5):738-45.
19. Cao MD, Nguyen SH, Ganesamoorthy D, Elliott AG, Cooper MA, Coin LJ. Scaffolding and completing genome assemblies in real-time with nanopore sequencing. Nat Commun. 2017;8:14515.
20. Harris PA, Taylor R, Thielke R, Payne J, Gonzalez N, Conde JG. Research electronic data capture (REDCap)--a metadata-driven methodology and workflow process for providing translational research informatics support. J Biomed Inform. 2009;42(2):377-81.
21. Institute CaLS. Perofrmance Standards for Antimicrobial Susceptiblity Testing. CLSI supplement M100. 2018.
22. Bolger AM, Lohse M, Usadel B. Trimmomatic: a flexible trimmer for Illumina sequence data. Bioinformatics. 2014;30(15):2114-20.
23. Bankevich A, Nurk S, Antipov D, Gurevich AA, Dvorkin M, Kulikov AS, et al. SPAdes: a new genome assembly algorithm and its applications to single-cell sequencing. J Comput Biol. 2012;19(5):455-77.
24. Kolmogorov M, Yuan J, Lin Y, Pevzner PA. Assembly of long, error-prone reads using repeat graphs. Nat Biotechnol. 2019;37(5):540-6.
25. Hunt M, Silva ND, Otto TD, Parkhill J, Keane JA, Harris SR. Circlator: automated circularization of genome assemblies using long sequencing reads. Genome Biol. 2015;16:294.
26. Vaser R, Sović, I., Nagarajan, N., & Šikić, M. Fast and accurate de novo genome assembly from long uncorrected reads. Genome research. 2017.
27. Page AJ, Cummins CA, Hunt M, Wong VK, Reuter S, Holden MT, et al. Roary: rapid large-scale prokaryote pan genome analysis. Bioinformatics. 2015;31(22):3691-3.
28. Löytynoja A. Phylogeny-aware alignment with PRANK. Totowa, NJ: Humana Press; 2014.
29. Stamatakis A. RAxML version 8: a tool for phylogenetic analysis and post-analysis of large phylogenies. Bioinformatics. 2014;30(9):1312-3.
30. Jolley KA, & Maiden, M. C. BIGSdb: scalable analysis of bacterial genome variation at the population level. BMC bioinformatics. 2010;11(1):595.
31. Seemann T. Prokka: rapid prokaryotic genome annotation. Bioinformatics. 2014;30(14):2068-9.

bioRxiv preprint doi: https://doi.org/10.1101/616961; this version posted March 19, 2020. The copyright holder for this preprint (which was not certified by peer review) is the author/funder. All rights reserved. No reuse allowed without permission.

907 32. Jia B, Raphenya AR, Alcock B, Waglechner N, Guo P, Tsang KK, et al. CARD 2017:
908 expansion and model-centric curation of the comprehensive antibiotic resistance database.
909 Nucleic Acids Res. 2017;45(D1):D566-D73.
910 33. Carattoli A, Zankari E, Garcia-Fernandez A, Voldby Larsen M, Lund O, Villa L, et al. In
911 silico detection and typing of plasmids using PlasmidFinder and plasmid multilocus sequence
912 typing. Antimicrob Agents Chemother. 2014;58(7):3895-903.
913 34. Siguier P, Perochon J, Lestrade L, Mahillon J, Chandler M. ISfinder: the reference centre
914 for bacterial insertion sequences. Nucleic Acids Res. 2006;34(Database issue):D32-6.
915 35. Hanson B, Johnson J, Leopold S, Sodergren E, Weinstock G. SVants – A long-read based
916 method for structural variation detection in bacterial genomes. bioRxiv. 2019:822312.
917 36. Dumas JL, van Delden C, Perron K, Kohler T. Analysis of antibiotic resistance gene
918 expression in Pseudomonas aeruginosa by quantitative real-time-PCR. FEMS Microbiol Lett.
919 2006;254(2):217-25.
920 37. Adler M, Anjum M, Berg OG, Andersson DI, Sandegren L. High fitness costs and
921 instability of gene duplications reduce rates of evolution of new genes by duplication-divergence
922 mechanisms. Mol Biol Evol. 2014;31(6):1526-35.
923 38. Gibson DG, Young L, Chuang RY, Venter JC, Hutchison CA, 3rd, Smith HO. Enzymatic
924 assembly of DNA molecules up to several hundred kilobases. Nature methods. 2009;6(5):343-5.
925 39. Partridge SR, Zong Z, Iredell JR. Recombination in IS26 and Tn2 in the evolution of
926 multiresistance regions carrying blaCTX-M-15 on conjugative IncF plasmids from Escherichia
927 coli. Antimicrob Agents Chemother. 2011;55(11):4971-8.
928 40. Sandegren L, Linkevicius M, Lytsy B, Melhus A, Andersson DI. Transfer of an
929 Escherichia coli ST131 multiresistance cassette has created a Klebsiella pneumoniae-specific
930 plasmid associated with a major nosocomial outbreak. J Antimicrob Chemother. 2012;67(1):74-
931 83.
932 41. Partridge SR. Analysis of antibiotic resistance regions in Gram-negative bacteria. FEMS
933 Microbiol Rev. 2011;35(5):820-55.
934 42. Partridge SR, Kwong, S. M., Firth, N., S.O. Mobile Genetic Elements Associated with
935 Antimicrobial Resistance. Clin Microbiol Rev. 2018;31(4):e00088-17.
936 43. He S, Hickman AB, Varani AM, Siguier P, Chandler M, Dekker JP, et al. Insertion
937 Sequence IS26 Reorganizes Plasmids in Clinically Isolated Multidrug-Resistant Bacteria by
938 Replicative Transposition. MBio. 2015;6(3):e00762.
939 44. Harmer CJ, Hall RM. IS26-Mediated Formation of Transposons Carrying Antibiotic
940 Resistance Genes. mSphere. 2016;1(2).
941 45. Harmer CJ, Moran RA, Hall RM. Movement of IS26-associated antibiotic resistance
942 genes occurs via a translocatable unit that includes a single IS26 and preferentially inserts
943 adjacent to another IS26. MBio. 2014;5(5):e01801-14.
944 46. Anantham S, Hall RM. pCERC1, a small, globally disseminated plasmid carrying the
945 dfrA14 cassette in the strA gene of the sul2-strA-strB gene cluster. Microb Drug Resist.
946 2012;18(4):364-71.
947 47. Boyd DA, Tyler S, Christianson S, McGeer A, Muller MP, Willey BM, et al. Complete
948 nucleotide sequence of a 92-kilobase plasmid harboring the CTX-M-15 extended-spectrum beta-
949 lactamase involved in an outbreak in long-term-care facilities in Toronto, Canada. Antimicrob
950 Agents Chemother. 2004;48(10):3758-64.
951 48. Iida S, Mollet B, Meyer J, Arber W. Functional characterization of the prokaryotic
952 mobile genetic element IS26. Molecular and General Genetics MGG. 1984;198(1):84-9.

bioRxiv preprint doi: https://doi.org/10.1101/616961; this version posted March 19, 2020. The copyright holder for this preprint (which was not certified by peer review) is the author/funder. All rights reserved. No reuse allowed without permission.

953 49. Harmer CJ, Hall RM. IS26-Mediated Precise Excision of the IS26-aphA1a
954 Translocatable Unit. MBio. 2015;6(6):e01866-15.
955 50. Livermore DM, Day M, Cleary P, Hopkins KL, Toleman MA, Wareham DW, et al.
956 OXA-1 beta-lactamase and non-susceptibility to penicillin/beta-lactamase inhibitor combinations
957 among ESBL-producing Escherichia coli. J Antimicrob Chemother. 2018.
958 51. Evans BA, Amyes SG. OXA beta-lactamases. Clin Microbiol Rev. 2014;27(2):241-63.
959 52. Evans SR, Hujer AM, Jiang H, Hujer KM, Hall T, Marzan C, et al. Rapid Molecular
960 Diagnostics, Antibiotic Treatment Decisions, and Developing Approaches to Inform Empiric
961 Therapy: PRIMERS I and II. Clin Infect Dis. 2016;62(2):181-9.
962 53. Bevan ER, Jones AM, Hawkey PM. Global epidemiology of CTX-M beta-lactamases:
963 temporal and geographical shifts in genotype. J Antimicrob Chemother. 2017;72(8):2145-55.
964 54. Mena A, Plasencia V, Garcia L, Hidalgo O, Ayestaran JI, Alberti S, et al.
965 Characterization of a large outbreak by CTX-M-1-producing Klebsiella pneumoniae and
966 mechanisms leading to in vivo carbapenem resistance development. J Clin Microbiol.
967 2006;44(8):2831-7.
968 55. Stoesser N, Sheppard AE, Pankhurst L, De Maio N, Moore CE, Sebra R, et al.
969 Evolutionary History of the Global Emergence of the Escherichia coli Epidemic Clone ST131.
970 mBio. 2016;7(2):e02162.
971 56. Poirel L, Lartigue M-F, Decousser J-W, Nordmann P. ISEcp1B-mediated transposition of
972 blaCTX-M in Escherichia coli. Antimicrobial agents and chemotherapy. 2005;49(1):447-50.
973 57. Zowawi HM, Forde BM, Alfaresi M, Alzarouni A, Farahat Y, Chong TM, et al. Stepwise
974 evolution of pandrug-resistance in Klebsiella pneumoniae. Sci Rep. 2015;5:15082.
975 58. Simner PJ, Antar AAR, Hao S, Gurtowski J, Tamma PD, Rock C, et al. Antibiotic
976 pressure on the acquisition and loss of antibiotic resistance genes in Klebsiella pneumoniae. J
977 Antimicrob Chemother. 2018;73(7):1796-803.
978 59. Hernández-Allés S, Benedí VJ, Martínez-Martínez L, Pascual Á, Aguilar A, Tomás JM,
979 et al. Development of resistance during antimicrobial therapy caused by insertion sequence
980 interruption of porin genes. Antimicrobial agents and chemotherapy. 1999;43(4):937-9.
981 60. Doumith M, Ellington MJ, Livermore DM, Woodford N. Molecular mechanisms
982 disrupting porin expression in ertapenem-resistant Klebsiella and Enterobacter spp. clinical
983 isolates from the UK. J Antimicrob Chemother. 2009;63(4):659-67.
984 61. Vandecraen J, Chandler M, Aertsen A, Van Houdt R. The impact of insertion sequences
985 on bacterial genome plasticity and adaptability. Crit Rev Microbiol. 2017;43(6):709-30.
986 62. Sandegren L, Andersson DI. Bacterial gene amplification: implications for the evolution
987 of antibiotic resistance. Nat Rev Microbiol. 2009;7(8):578-88.
988 63. Andersson DI, Hughes D. Antibiotic resistance and its cost: is it possible to reverse
989 resistance? Nat Rev Microbiol. 2010;8(4):260-71.
990 64. Leavitt A, Chmelnitsky I, Colodner R, Ofek I, Carmeli Y, Navon-Venezia S. Ertapenem
991 resistance among extended-spectrum-beta-lactamase-producing Klebsiella pneumoniae isolates.
992 J Clin Microbiol. 2009;47(4):969-74.
993 65. Nicoloff H, Hjort K, Levin BR, Andersson DI. The high prevalence of antibiotic
994 heteroresistance in pathogenic bacteria is mainly caused by gene amplification. Nat Microbiol.
995 2019;4(3):504-14.
996 66. Gullberg E, Albrecht LM, Karlsson C, Sandegren L, Andersson DI. Selection of a
997 multidrug resistance plasmid by sublethal levels of antibiotics and heavy metals. mBio.
998 2014;5(5):e01918-14.

bioRxiv preprint doi: https://doi.org/10.1101/616961; this version posted March 19, 2020. The copyright holder for this preprint (which was not certified by peer review) is the author/funder. All rights reserved. No reuse allowed without permission.

999 67. Andersson DI, Nicoloff H, Hjort K. Mechanisms and clinical relevance of bacterial
1000 heteroresistance. Nat Rev Microbiol. 2019;17(8):479-96.
1001